Ventilation-Perfusion Scan: A Primer for Practicing Radiologists

Paul-Robert Derenoncourt, MD
Gabriel J. Felder, MD
Henry D. Royal, MD
Sanjeev Bhalla, MD
Jordan A. Lang, MD
Manuela C. Matesan, MD
Malak Itani, MD

Lung scintigraphy, or ventilation-perfusion (V/Q) scan, is one of the commonly performed studies in nuclear medicine. Owing to variability in clinical applications and different departmental workflows, many trainees are not comfortable interpreting the results of this study. This article provides a simplified overview of V/Q imaging, including a review of its technique, interpretation methods, and established and emerging clinical applications. The authors review the role of V/Q imaging in evaluation of acute and chronic pulmonary embolism, including the role of SPECT/CT and comparing V/Q scan with CT angiography. In addition, a variety of other applications of pulmonary scintigraphy are discussed, including congenital heart disease, pretreatment planning for lung cancer and emphysema, posttransplant imaging for bronchiolitis obliterans, and less common vascular and nonvascular pathologic conditions that may be detected with V/Q scan. This article will help radiologists and residents interpret the results of V/Q scans and understand the various potential clinical applications of this study.

Online supplemental material is available for this article.

Abbreviations: CHD = congenital heart disease, COPD = chronic obstructive pulmonary disease, CTPA = CT pulmonary angiography, DTPA = diethylenetriaminepentaacetic acid, EANM = European Association of Nuclear Medicine, MAA = macroaggregated albumin, PE = pulmonary embolism, PIOPED = Prospective Investigation of Pulmonary Embolism Diagnosis, PISAPED = Prospective Investigative Study of Acute Pulmonary Embolism Diagnosis, V/Q = ventilation-perfusion

RadioGraphics 2021; 41:2047–2070

https://doi.org/10.1148/rg.2021210060

Content Codes: CH NM

From the Mallinckrodt Institute of Radiology, Washington University in St Louis, 510 S Kingshighway Blvd, Campus Box 8131, St Louis, MO 63110 (P.R.D., H.D.R., S.B., J.A.L., M.I.); Department of Radiology, NYU Winthrop Hospital, Mineola, NY (G.J.F.); and Department of Radiology, University of Washington Medical Center, Seattle, Wash (M.C.M.). Recipient of a Certificate of Merit award for an education exhibit at the 2020 RSNA Annual Meeting. Received March 13, 2021; revision requested April 20 and received April 30; accepted May 7. For this journal-based SA-CME activity, the authors, editor, and reviewers have disclosed no relevant relationships. **Address correspondence to** M.I. (e-mail: *mitani@wustl.edu*).

SA-CME LEARNING OBJECTIVES

After completing this journal-based SA-CME activity, participants will be able to:

- Describe various techniques and tracers used in V/Q imaging.
- Familiarize physicians with methods and guidelines available, and provide easy-to-follow instructions, for interpreting VQ scans in the setting of PE.
- List additional clinical applications of V/Q scan apart from evaluating for PE.

See rsna.org/learning-center-rg.

Introduction

Ventilation-perfusion (V/Q) scintigraphy is the oldest noninvasive radiologic examination available for evaluating pulmonary embolism (PE); its initial use in humans for this purpose was reported in 1964 by Quinn et al (1). It was not until 1978 that PE was reported at CT (2). Because V/Q scintigraphy is an old technique, several interpretation algorithms have been proposed and are in use, but the most accurate interpretation method for planar V/Q imaging remains the gestalt method, which highly depends on reader experience (3).

During the 1980s, several interpretation criteria were proposed, including the McNeil (4), Biello (5), and Prospective Investigation of Pulmonary Embolism Diagnosis (PIOPED) (6) criteria. Continued efforts to improve the diagnostic performance of V/Q scintigraphy included PIOPED II (7), the perfusion-only Prospective Investigative Study of Acute Pulmonary Embolism Diagnosis (PISAPED) (8), and the European Association of Nuclear Medicine (EANM) guidelines, which strongly preferred imaging with SPECT (9).

TEACHING POINTS

- Triple matches in the lower lobes are more likely to be due to PE than triple matches in the upper lobes.
- An uncommon finding at V/Q scan is unilateral lung hypoperfusion, which is unlikely to represent PE (<2% of cases).
- A positive V/Q study is not specific for acute PE and can be seen with chronic PE, so reviewing prior V/Q studies if available is important.
- The posttest probability of disease is determined by combining the test result with the pretest probability of disease.
- Lung scan is more appropriate than CTPA for detecting chronic thromboembolic pulmonary disease as a cause of pulmonary hypertension.

The purpose of this article is to *(a)* propose a logical framework for radiology and nuclear medicine residents and physicians to interpret results of V/Q studies and *(b)* present the various clinical applications of V/Q imaging with a focus on PE evaluation using probabilistic methods, discussing their applicability and limitations.

V/Q Scintigraphy Technique

A V/Q scan consists of two portions, the V or ventilation portion and the Q or perfusion portion (Table 1). Anecdotally, *Q*—for quantity—was used by French scientists to refer to blood flow rate and was thus kept as an abbreviation for perfusion. The perfusion portion of the study is occasionally performed without the ventilation portion (10).

With the COVID-19 pandemic, many institutions have shifted to perfusion-only imaging in patients with suspected PE who have suspected or documented COVID-19 infection, owing to concern about the transmissibility of COVID-19 with ventilation systems. The recommendation to forgo ventilation imaging, whenever feasible, during the pandemic is supported by guidance statements from the Society of Nuclear Medicine and Molecular Imaging (SNMMI) (11), as well as the American College of Radiology (ACR) (12).

Ventilation

There are two types of ventilation radiopharmaceuticals: aerosols and inert gases. Aerosols are suspensions of very fine particles, with a median diameter range of 0.1–5 μm, that are deposited in the alveoli (13,14). The most commonly used aerosol is technetium 99m (^{99m}Tc)–diethylenetriaminepentaacetic acid (DTPA) (15), which is a liquid aerosol. An ultrafine dispersion of ^{99m}Tc-labeled carbon is made of solid graphite particles (Technegas; Cyclomedica) with a median diameter of 0.158 μm and provides a more uniform distribution than liquid aerosols, but it is not yet approved by the U.S. Food and Drug Administration (FDA) for use in the United States (14).

DTPA aerosol is administered using a mouthpiece during tidal breathing, preferably with the patient upright. Twenty-five to 35 mCi (925–1295 MBq) of ^{99m}Tc-DTPA is placed in the nebulizer, resulting in a delivered or deposited activity of less than 2.0 mCi (74 MBq) in the lungs. Once it is deposited in the alveoli, the distribution of aerosols in the lung is relatively static. ^{99m}Tc-DTPA aerosol stays in the lungs long enough (effective half-life of 1 hour) for acquisition of multiple planar projections and/or performance of SPECT (16). Technegas has a longer effective half-life (about 6 hours) (9), and its distribution in the lung is also relatively static.

Typically acquired projections for planar images are anterior, posterior, right and left lateral, and right and left anterior and posterior oblique views. Given the relatively large size of the ^{99m}Tc-DTPA aerosolized liquid particles compared with those of Technegas, there is more central airway deposition of the aerosol; this limits the accuracy of quantification with ^{99m}Tc-DTPA (Fig 1). Other factors contributing to central airway deposition include turbulent flow such as in chronic obstructive pulmonary disease (COPD), and tachypnea.

Inert gases, or noble gases, are a class of elements that do not form chemical reactions. Xenon 133 (^{133}Xe) is the only inert gas available for ventilation scintigraphy in the United States (17). ^{133}Xe is inhaled as a mixture with oxygen or air, in a variable concentration depending on the patient's oxygenation needs; the inhaled dose is usually 5–20 mCi (185–740 MBq), all of which is exhaled with a biologic half-life of 30 seconds, resulting in a small effective dose (17).

A facemask or mouthpiece is connected to the xenon delivery system (Fig E1). The patient takes a single breath to end-inspiratory capacity first and tries to hold it for 20 seconds while a single-breath image is obtained, then wash-in or equilibrium images (typically 2–3 minutes) are obtained while the patient re-breathes the xenon and air in a closed system. Finally, washout images (2–3 minutes) are acquired.

Xenon provides the best physiologic evaluation of ventilation and is more sensitive for obstructive airway disease (15). Single-breath wash-in images demonstrate ventilation defects (areas of decreased activity) before any collateral ventilation sets in, while washout phase images are most sensitive for areas of air trapping in obstructive airway disease (18).

Because there is no central airway deposition, xenon images provide quantitative information about the patient's ventilation. The disadvantage

Table 1: Radiopharmaceuticals Used in V/Q Scans

Type of Agent	Isotope Half-life	Main Photon Energy (keV)*
Ventilation agents		
^{99m}Tc-DTPA aerosol	6 h	140 (224 × 10^{-16})
^{99m}Tc-Technegas†	6 h	140 (224 × 10^{-16})
^{133}Xe gas	5.27 d	81 (130 × 10^{-16})
^{81m}Kr gas	13 sec	190 (304 × 10^{-16})
Perfusion agents		
^{99m}Tc-MAA	6 h	140 (224 × 10^{-16})

Note.—DTPA = diethylenetriaminepentaacetic acid, ^{81m}Kr = krypton 81m, MAA = macroaggregated albumin, ^{99m}Tc = technetium 99m, ^{133}Xe = xenon 133.
*Numbers in parentheses are values in SI units (joules).
†Graphite ultrafine particles (Cyclomedica).

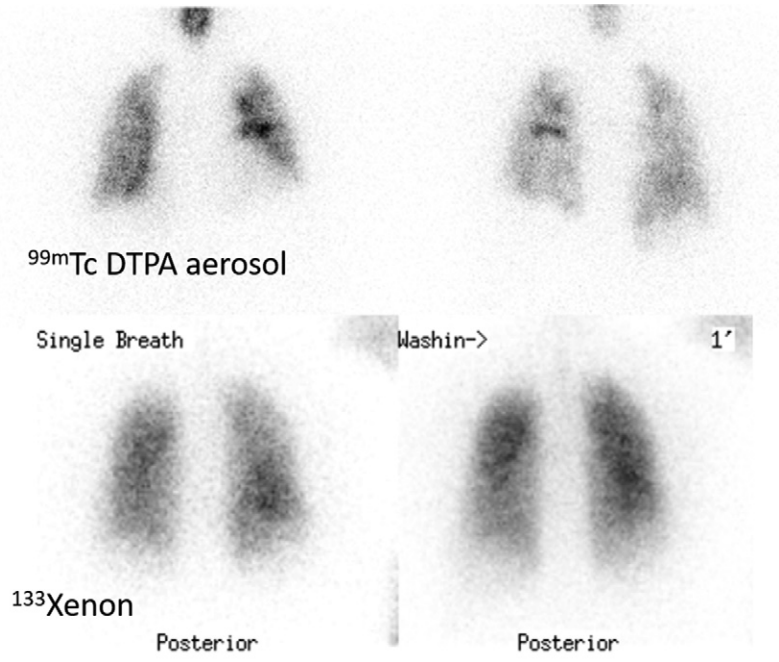

Figure 1. ^{99m}Tc-DTPA aerosol ventilation scan compared with ^{133}Xe ventilation scan in a 68-year-old man with chronic myelogenous lymphoma and hypoxemia. Top: Anterior and posterior ventilation images with ^{99m}Tc-DTPA aerosol show markedly heterogeneous tracer deposition. Bottom: Xenon images (posterior projection only) show less heterogeneity and more uniform deposition.

of xenon studies is that, for radiation safety reasons, they have to be performed in a negative-pressure room with an appropriate exhaust system in case of a radioactive gas leak. Therefore, unlike studies with ^{99m}Tc-DTPA inhaled aerosol, xenon studies cannot be performed portably.

Because the distribution of the xenon in the lung is constantly changing during the study, images can be obtained only in limited projections. SPECT cannot usually be performed with xenon. Another disadvantage of xenon is suboptimal image quality due to the low photopeak (81 keV [130 × 10^{-16} J]) and poor image count rate (19). Of note, a commonly seen nonpulmonary abnormality at xenon perfusion imaging is tracer accumulation or retention in the liver, seen with hepatic steatosis (Fig E2).

Perfusion

^{99m}Tc–macroaggregated albumin (MAA) is used as the perfusion agent in V/Q scan. It is injected intravenously and slowly over four to five respiratory cycles, after the vial is agitated and the syringe is inverted to avoid the settled particles. Care should be taken not to withdraw any blood into the syringe before the injection, to avoid forming clots that result in foci of concentrated tracer, resulting in imaging artifacts (Fig E3). Similar clot labeling has been described in a patient injected in an upper extremity affected by thrombophlebitis (20).

^{99m}Tc-MAA has a biologic half-life of 1.5–3 hours in the lungs, allowing acquisition of multiple planar images and performance of SPECT. A range of 1–4 mCi (37–148 MBq) of activity is

administered; a 3-mCi (111-MBq) dose results in an approximate effective dose of 1.2 mSv in an average adult (15,17). Ideally, the patient is injected while supine to minimize the vertical perfusion gradient and decrease diaphragmatic motion, and the dose is given in 200 000 to 700 000 particles (9,15). The particles are slightly larger than red blood cells, with a size range of 5–100 μm (most are 10–30 μm), causing microemboli to an estimated 0.1% of the pulmonary precapillary arterioles.

In patients with pulmonary hypertension or right-to-left shunt, the same administered activity should be given with a reduced number of particles of 100 000–200 000 (15). Owing to the particle size, ^{99m}Tc-MAA injection should not be performed in a central line with an in-line filter. In patients undergoing extracorporeal membrane oxygenation (ECMO), intravenously injected ^{99m}Tc-MAA radiopharmaceutical can be partially or totally shunted to the machine then to the systemic circulation (Fig E4) (21); therefore, if clinically possible, ECMO should be stopped for a minute or so at the time of the injection.

A reduction in administered activity might be needed in pregnant or pediatric patients. In patients with congenital heart disease (CHD), the site of tracer injection should be carefully planned, depending on the patient's circulation; for example, lower limb injection is required for evaluating an intracardiac shunt after the bidirectional Glenn procedure. A slightly higher dose—typically 5 mCi (185 MBq) instead of 4 mCi (148 MBq)—is needed for the perfusion scan if a ^{99m}Tc aerosol is used earlier for ventilation, so that the count rate after the MAA injection increases by a factor of four to six times.

SPECT/CT

The relationship of SPECT to planar imaging is similar to that of CT compared with radiography, except that imaging is performed with a gamma camera, which is rotated slowly to acquire one image after every few degrees of rotation. SPECT provides higher contrast resolution and three-dimensional visualization, which allows better characterization and localization of perfusion defects and better matching with aerosol ventilation defects.

When CT is also performed, SPECT/CT allows even better anatomic localization—with imaging findings that can be confirmatory for PE, such as hyperattenuating clot or differential vessel size—or demonstrates an alternative cause to explain the patient's symptoms, such as pneumonia, pulmonary edema, or another pathologic condition. The EANM recommends use of V/Q SPECT in lung scintigraphy and strongly recommends SPECT/CT for perfusion imaging.

Correlative Imaging for Lung Scintigraphy

Guidelines of the Society of Nuclear Medicine and Molecular Imaging (SNMMI) recommend radiographic evaluation—typically posteroanterior and lateral chest radiography—as part of patient preparation for V/Q scan, but CT can substitute (Fig 2). This is usually performed within 24 hours before the lung scintigraphy, but radiographic evaluation performed within a few days earlier is adequate if the patient has no acute change of symptoms. If the patient has acute onset of symptoms, more recent chest radiography may be needed. The role of anatomic imaging is to detect thoracic abnormalities that could explain perfusion or ventilation defects. Some studies suggest that chest radiography can reliably replace the ventilation portion of the V/Q scan, especially in the younger population and those without obstructive airway disease (22–24).

Evaluation of PE

Lung scintigraphy has been used for decades for diagnosis of PE. In addition, lung scintigraphy can be used to evaluate clot burden in the lung and clot resolution and for evaluation of patients with pulmonary hypertension (25–28).

Historically, interpretation of V/Q studies for diagnosis of PE is based on probabilistic methods (Bayes theorem). To determine the posttest probability of disease (how often a patient with a positive test actually has the disease), the results of the imaging test (V/Q scan) are combined with the pretest probability of disease (the estimate of the disease in the population that is studied). As such, the pretest probability is extremely important in determining the appropriateness of the test and in the posttest probability of having PE.

The pretest probability can be determined on the basis of the clinical manifestation and the D-dimer level. The Wells score is a clinical prediction score for determining the pretest probability of acute PE to help decide which patients require further investigations (29). Managing patients on the basis of the Wells score pretest probability (Table 2) and the D-dimer result is safe and decreases the need for diagnostic imaging, but high clinical suspicion should always take precedence (29).

The Geneva score, modified in 2006, is another tool for evaluating the pretest probability of PE (30). A common algorithm used is that if the patient has a Wells score of 4 or less and the D-dimer test is negative, no further testing is neces-

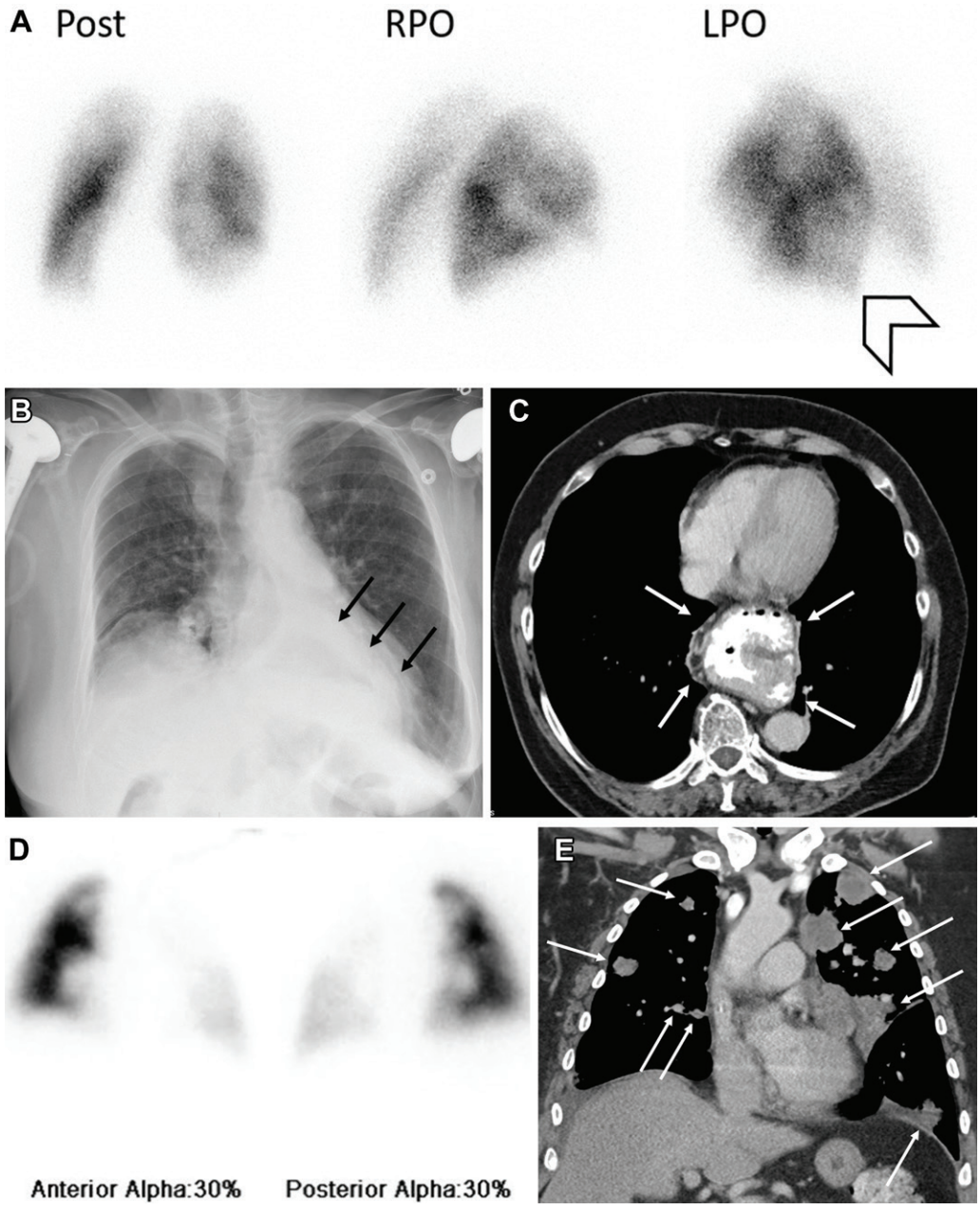

Figure 2. Role of correlative anatomic imaging in two patients. **(A–C)** A 75-year-old woman with increasing oxygen requirements after shoulder surgery. **(A)** Perfusion images show a large area of decreased perfusion in the left lung base medially (arrowhead), best appreciated on the left posterior oblique *(LPO)* view. *Post* = posterior, *RPO* = right posterior oblique. **(B)** Correlative radiograph obtained on the same day shows a retrocardiac opacity with an air-fluid level (arrows), consistent with a hiatal hernia, which corresponds to the perfusion defect. **(C)** Axial CT image also shows the hiatal hernia (arrows). **(D, E)** A 63-year-old man with spindle cell carcinoma of the left groin metastatic to the lungs who presented with shortness of breath. **(D)** Lung perfusion scan shows numerous areas of markedly decreased perfusion, with significantly reduced unilateral perfusion to the entire left lung. **(E)** On a coronal CT image, the perfusion defects correspond to numerous metastatic deposits (arrows). The patient also had complete occlusion of the left superior and inferior pulmonary veins (not shown).

sary; a score greater than 4 would require further investigation (31). On the basis of the American College of Radiology (ACR) appropriateness criteria (32), V/Q scan or alternatively CT pulmonary angiography (CTPA) is usually appropriate in the setting of suspected PE with intermediate pretest probability and positive D-dimer test or high pretest probability.

ABCs of Interpretation

Chest radiography is the study of choice for initial evaluation of patients with suspected PE and is used for correlation, as detailed earlier (32). Interpretation of lung scintigraphy results for PE should begin with careful evaluation of the perfusion images, a schema that allows perfusion-only imaging in select patients. The pulmonary

Table 2: Wells Criteria and Modified Wells Criteria

Clinical Features	Attributable Points*
Clinical symptoms of DVT†	3
Other diagnosis less likely than PE	3
Tachycardia (heart rate >100 beats per minute)	1.5
Immobilization for ≥3 days or surgery in past 4 weeks	1.5
Previous DVT or PE	1.5
Hemoptysis	1
Malignancy	1

*Wells criteria: high probability >6, moderate probability 2–6, low probability <2. Modified Wells criteria: PE likely >4, PE unlikely ≤4.
†DVT = deep vein thrombosis. Clinical symptoms include leg swelling and pain.

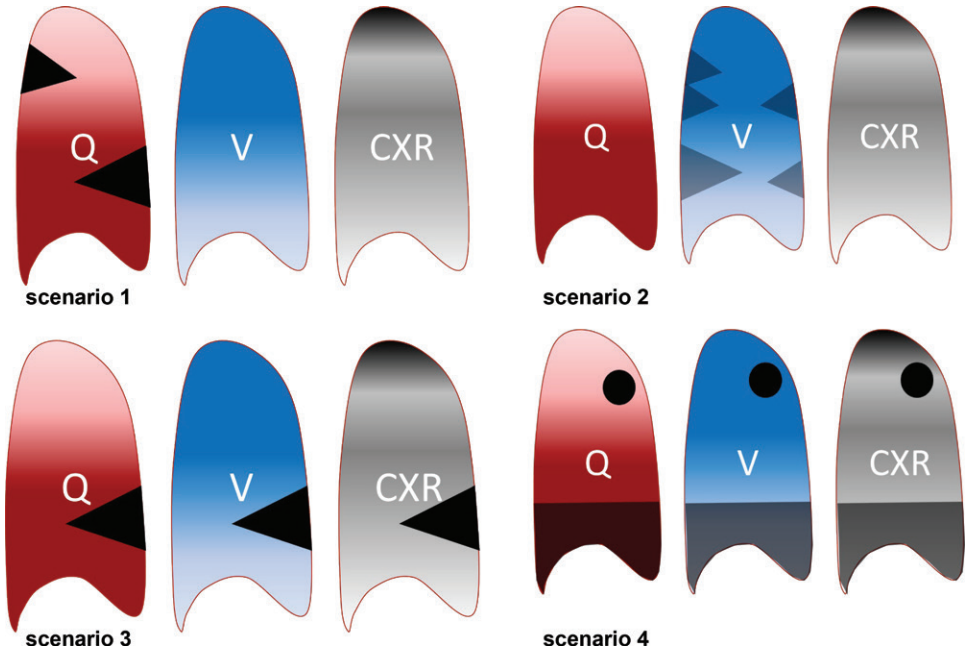

Figure 3. Schematic guide to interpretation of V/Q scans. If perfusion *(Q)* images are normal, then there is no PE. Scenario 1: If perfusion images show two or more large defects, or their equivalent, with normal or better ventilation *(V)* and normal appearance or smaller abnormality at chest radiography *(CXR)*, then there is high probability of PE. Scenario 2: Ventilation abnormalities with normal perfusion and normal or near-normal chest radiographs represent a reverse mismatch and are a classic appearance of airway disease such as chronic obstructive pulmonary disease (COPD). Scenarios 3 and 4: A defect that is matched on perfusion and ventilation images may or may not have a corresponding radiographic abnormality and is usually not a PE. This can be segmental or lobar (eg, in pneumonia) (scenario 3) or have round or smooth margins in cases of tumors or pleural effusions (scenario 4).

arteries provide 99% of the blood flow to the lungs, with lobar arteries dividing into segmental arteries then subsegmental terminal arteries with no collateralization. The bronchial arteries supply only 1% of the blood flow to the lungs to nourish the supporting structures (33). This arterial anatomy forms the basis of the lung perfusion scan, and the end-artery supply is the reason why PE results in wedge-shaped defects that are narrow centrally and broad peripherally, seen on perfusion images (Q scans) as perfusion defects.

As a result, we suggest that the first step in evaluating V/Q studies is to track the lung periphery on the perfusion images; if this is continuous and conforms to the normal expected contour, then there is no PE, regardless of any other findings in the study (Fig 3). If the perfusion images are not normal, then ventilation images and radiologic evaluation come into play (34). The typical finding of PE at V/Q scan is a mismatched perfusion defect, since perfusion is absent or reduced but ventilation is still normal (Figs 4, E5).

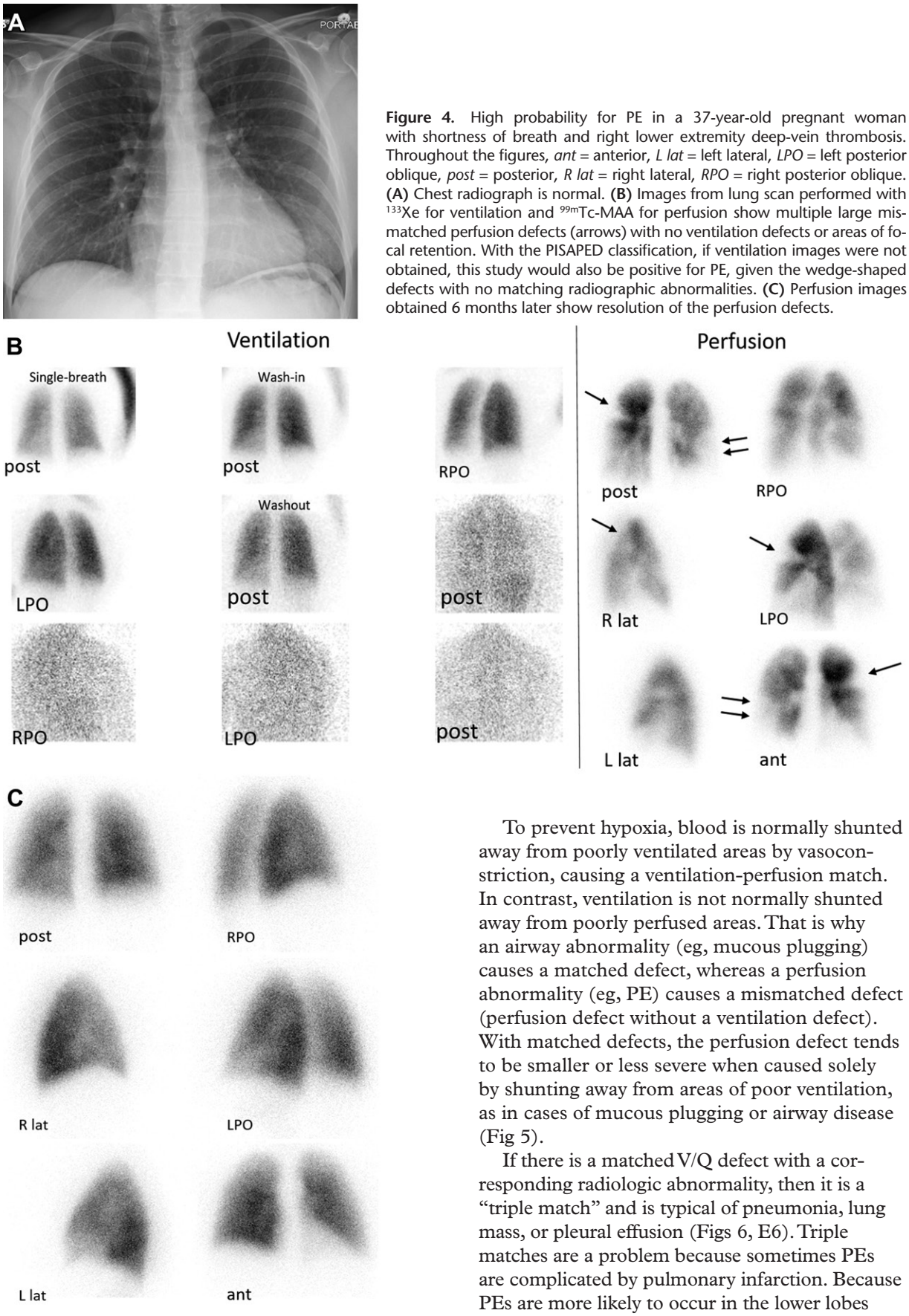

Figure 4. High probability for PE in a 37-year-old pregnant woman with shortness of breath and right lower extremity deep-vein thrombosis. Throughout the figures, *ant* = anterior, *L lat* = left lateral, *LPO* = left posterior oblique, *post* = posterior, *R lat* = right lateral, *RPO* = right posterior oblique. **(A)** Chest radiograph is normal. **(B)** Images from lung scan performed with ^{133}Xe for ventilation and ^{99m}Tc-MAA for perfusion show multiple large mismatched perfusion defects (arrows) with no ventilation defects or areas of focal retention. With the PISAPED classification, if ventilation images were not obtained, this study would also be positive for PE, given the wedge-shaped defects with no matching radiographic abnormalities. **(C)** Perfusion images obtained 6 months later show resolution of the perfusion defects.

To prevent hypoxia, blood is normally shunted away from poorly ventilated areas by vasoconstriction, causing a ventilation-perfusion match. In contrast, ventilation is not normally shunted away from poorly perfused areas. That is why an airway abnormality (eg, mucous plugging) causes a matched defect, whereas a perfusion abnormality (eg, PE) causes a mismatched defect (perfusion defect without a ventilation defect). With matched defects, the perfusion defect tends to be smaller or less severe when caused solely by shunting away from areas of poor ventilation, as in cases of mucous plugging or airway disease (Fig 5).

If there is a matched V/Q defect with a corresponding radiologic abnormality, then it is a "triple match" and is typical of pneumonia, lung mass, or pleural effusion (Figs 6, E6). Triple matches are a problem because sometimes PEs are complicated by pulmonary infarction. Because PEs are more likely to occur in the lower lobes (because of increased blood flow), triple matches in the lower lobes are more likely to be due to PE than triple matches in the upper lobes (35).

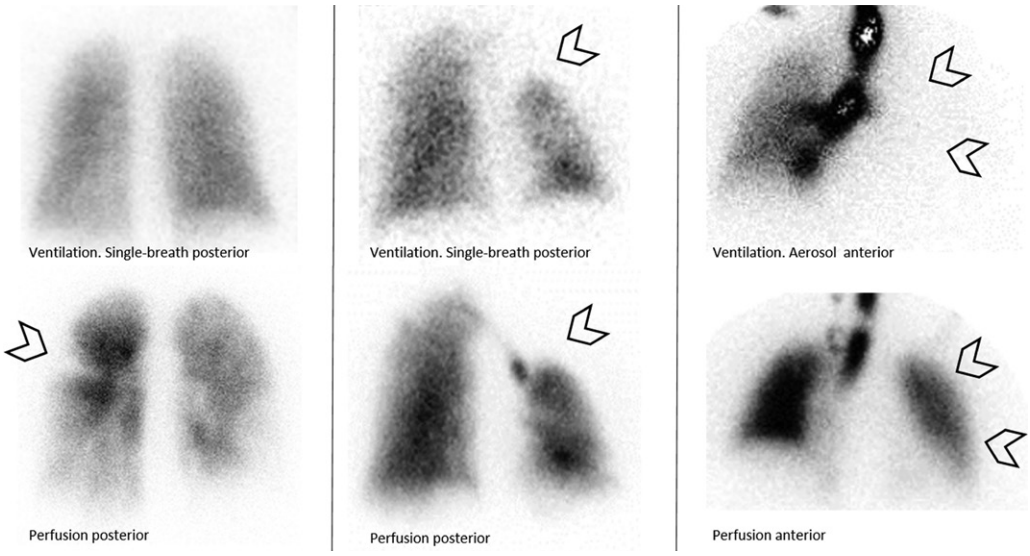

Figure 5. Mismatched, matched, and reverse-mismatched defects. Left: V/Q images show a triangular perfusion defect (arrowhead) with no corresponding ventilation defect (mismatched perfusion defect). Center: V/Q images show a perfusion defect that is not triangular (bottom arrowhead) and corresponds to a similar ventilation defect (top arrowhead) (nonsegmental matched defect). Right: V/Q images show a ventilation defect with absent ventilation of the left lung (top arrowheads) but preserved perfusion (bottom arrowheads) (reverse-mismatched defect).

Figure 6. Intermediate probability for PE in a 66-year-old man with shortness of breath after bilateral lung transplant. **(A)** Chest radiograph shows a small right pleural effusion in addition to peripheral consolidations in the right mid and bilateral lower lung zones. **(B)** Images from lung scintigraphy performed with ^{133}Xe for ventilation and ^{99m}Tc-MAA for perfusion demonstrate an intermediate probability for PE, given the one nonsegmental right lower lobe triple-matched ventilation and perfusion defect corresponding to the known radiographic abnormality. With the PISAPED classification, if ventilation images were not obtained, this study would be abnormal but negative for PE, given that the perfusion defect is non–wedge-shaped and corresponds to a matching radiographic abnormality.

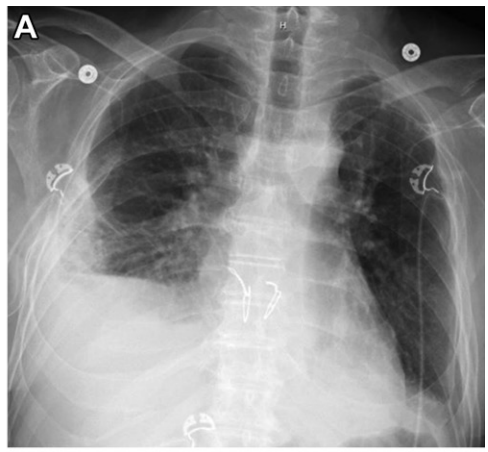

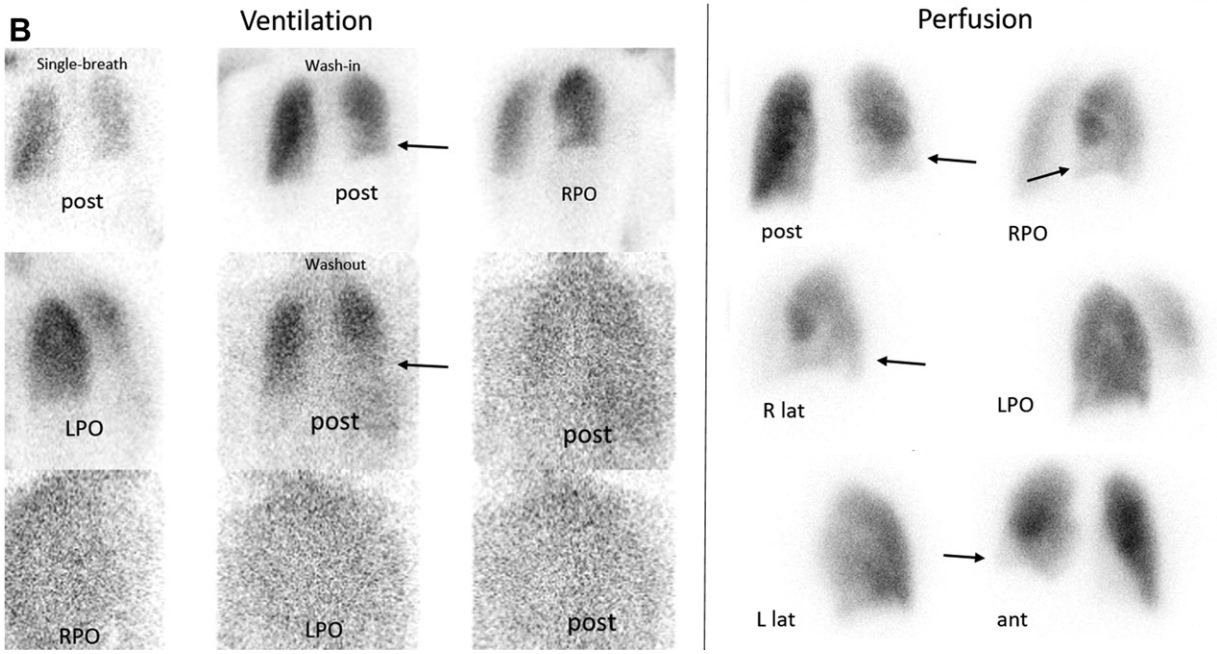

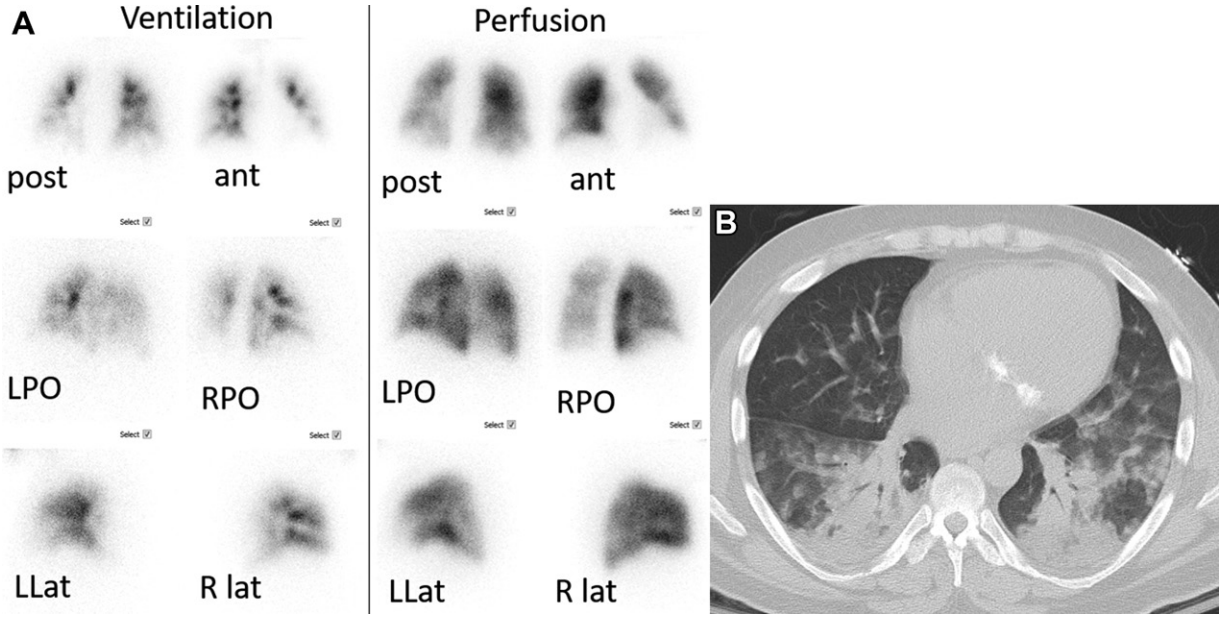

Figure 7. Low probability for PE in a 41-year-old man with hypoxia, tachycardia, and hypotension 2 days after renal transplant. **(A)** V/Q images obtained with ^{99m}Tc-DTPA aerosol for ventilation and ^{99m}Tc-MAA for perfusion show multiple peripheral areas of decreased ventilation, worse in the lower lobes, with better or preserved perfusion. **(B)** Axial CT image obtained on the same day shows multifocal consolidations and ground-glass infiltrates, worse in the lower lobes, consistent with pneumonia.

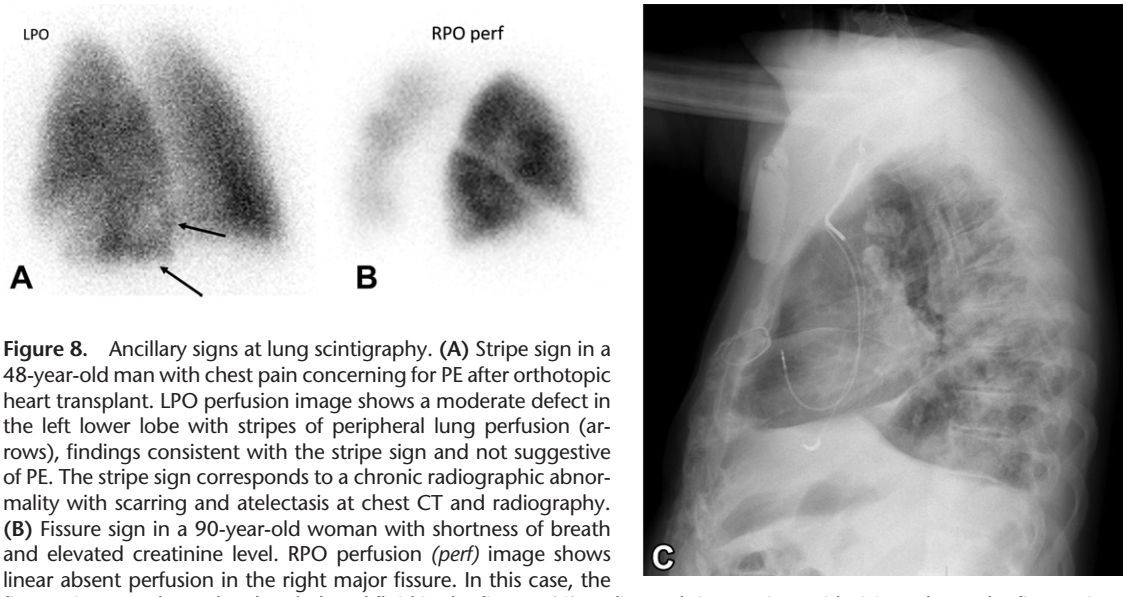

Figure 8. Ancillary signs at lung scintigraphy. **(A)** Stripe sign in a 48-year-old man with chest pain concerning for PE after orthotopic heart transplant. LPO perfusion image shows a moderate defect in the left lower lobe with stripes of peripheral lung perfusion (arrows), findings consistent with the stripe sign and not suggestive of PE. The stripe sign corresponds to a chronic radiographic abnormality with scarring and atelectasis at chest CT and radiography. **(B)** Fissure sign in a 90-year-old woman with shortness of breath and elevated creatinine level. RPO perfusion *(perf)* image shows linear absent perfusion in the right major fissure. In this case, the fissure sign was due to loculated pleural fluid in the fissure. **(C)** Radiograph in a patient with COPD shows the fissure sign, which was due to fissural pleural thickening in this case.

When a ventilation defect is present in a segment with normal or much better perfusion, it is described as a functional right-to-left shunt ("reverse mismatch"). Functional right-to-left shunting is commonly seen with pneumonia or mucous plugging. It explains the patient's hypoxia and often results in changes in patient management (Fig 7).

Certain imaging findings—such as a stripe of perfused lung between a perfusion defect and the adjacent pleural surface (stripe sign) or linear defects conforming to the shape and location of the fissure (fissure sign)—favor causes other than PE (Fig 8). An uncommon finding at V/Q scan is unilateral lung hypoperfusion, which is unlikely to represent PE (<2% of cases) (36) and is commonly caused by mass effect on the pulmonary artery at the hilum, usually from lung cancer, pleural conditions (effusion, fibrothorax, trapped lung), asymmetric parenchymal diseases (bullous emphysema), postinflammatory conditions (fibrosing mediastinitis, Swyer-James syndrome),

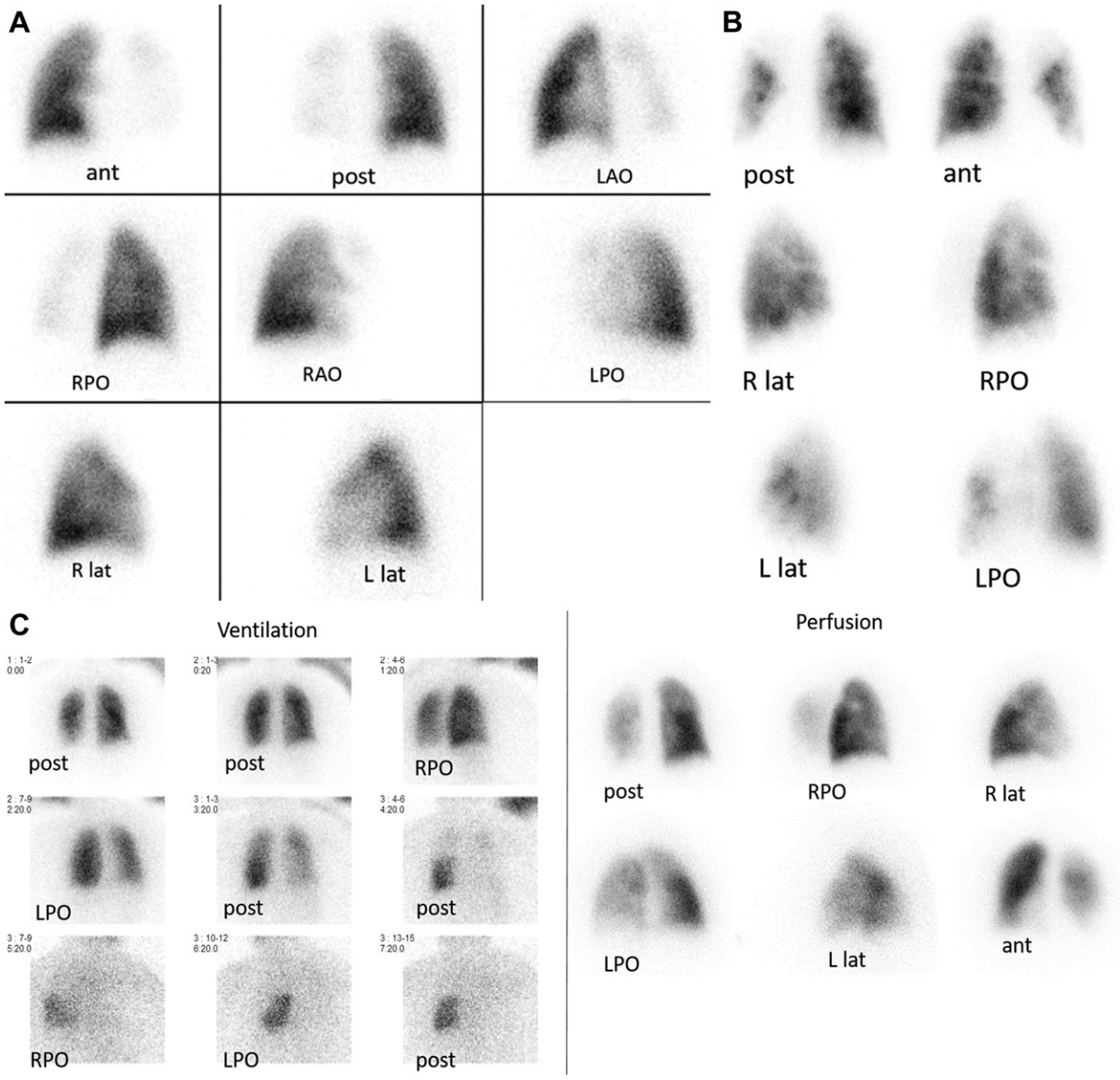

Figure 9. Unilateral lung hypoperfusion in different patients. **(A)** A 12-year-old girl after repair of tetralogy of Fallot. Images from perfusion lung scintigraphy show markedly decreased heterogeneous perfusion of the left lung and normal perfusion of the right lung. The hypoperfusion was secondary to left pulmonary artery hypoplasia, seen at echocardiography. Throughout the figures, *LAO* = left anterior oblique, *RAO* = right anterior oblique. **(B)** A 46-year-old man with longstanding Swyer-James syndrome who underwent evaluation for lung transplant. Images from perfusion lung scintigraphy show severe hypoperfusion of the left lung. **(C, D)** A patient with left lower lobe congenital pulmonary hypoplasia secondary to congenital diaphragmatic hernia. Xenon ventilation images **(C)** and coronal CT image **(D)** show severe air trapping in the left lower lobe.

iatrogenic changes (from radiation therapy, pneumonectomy, lung transplant), or congenital anomalies (pulmonary artery hypoplasia or sling) (36) (Fig 9). Nevertheless, if there are multiple contralateral segmental large or moderate-sized mismatched perfusion defects, suspicion should be high for PE.

Note that V/Q scan does not demonstrate the age of a PE; it demonstrates only its presence. A positive V/Q study is not specific for acute PE and can be seen with chronic PE, so reviewing prior V/Q studies if available is important.

Criteria for Diagnosis

For planar V/Q imaging, interpretation is based on probabilistic methods defined by interpretation systems. The most widely used are the PIOPED criteria (6), which were updated to

Table 3: Modified PIOPED II Criteria

Interpretation	Imaging Findings*
High probability (PE present)	≥two large segmental mismatched defects (two moderate defects = one large defect)
Normal perfusion or very low probability (PE absent)	Nonsegmental perfusion defects Perfusion defect smaller than corresponding CXR finding One to three small segmental defects ≥matched V/Q defects with regionally normal CXR and areas of normal perfusion elsewhere in lung Solitary triple-matched defect in mid and upper lung zone confined to a single segment Stripe sign Pleural effusion of one-third or more of pleural cavity with no other perfusion defect in either lung
Low or intermediate probability (nondiagnostic)	All other findings Per PIOPED I, low probability: Nonsegmental perfusion defects (reclassified into very low probability) Single moderate mismatched segmental perfusion defect with normal CXR Any perfusion defect with substantially larger CXR abnormality Large or moderate segmental perfusion defects (≤four segments in one lung and ≤three segments in one lung region) with matching or larger ventilation defects, with or without CXR abnormalities (substantially smaller than perfusion defects) >three small segmental perfusion defects with normal CXR

*CXR = chest radiography.

PIOPED II (6), then revised into the modified PIOPED II (mPIOPED II) to reduce the number of nondiagnostic studies (15,37); less common interpretation guidelines include the McNeil and Biello criteria (4,5). When the ventilation scan is not performed, Q scan interpretation systems are the perfusion-only modified PIOPED II (pPIOPED II) and PISAPED (8,23).

In addition to the shape, the size of a defect is of paramount importance. A large defect occupies more than 75% of a segment, a moderate-sized defect occupies 25%–75%, and a small defect occupies less than 25%. An overview of mPIOPED II and PISAPED is presented in Tables 3 and 4.

In a sample of 910 patients with a PE prevalence of 18% (168 of 910), use of mPIOPED II resulted in sensitivity of 77% (95% CI: 70%, 85%) for the PE-present category (or the ability of a high-probability scan to demonstrate PE) and specificity of 98% (95% CI: 96%, 99%) for the PE-absent category (or the ability of a very low–probability or normal scan to exclude PE), using a composite reference standard of digital subtraction angiography, CT angiography, and Wells score (37).

In a sample of 889 patients with a PE prevalence of 19% (169 of 889), use of pPIOPED II or PISAPED with chest radiography yielded accuracy comparable to that of V/Q scan and of CTPA, with sensitivity for a PE-present result (positive perfusion scan) of 85% (95% CI: 80%, 89%) with pPIOPED II and 80% (95% CI: 76%, 84%) with PISAPED and specificity for a PE-absent result (negative perfusion scan) of 93% (95% CI: 91%, 94%) with pPIOPED II and 97% (95% CI: 96%, 97%) with PISAPED, although the main difference was that pPIOPED II resulted in 20.6% nondiagnostic studies compared with 0% for PISAPED (23).

The posttest probability of disease is determined by combining the test result with the pretest probability of disease. If V/Q scan is performed in a population of low-clinical-likelihood patients, the posttest probability of disease (or percentage of true positives) will be much lower than if the test is performed in a population of high-clinical-likelihood patients. The importance of the clinical pretest probability is emphasized by demonstrating the stratified outcome variability in patients in the intermediate-probability category. In the original PIOPED study, the overall prevalence of PE in patients with intermediate-probability V/Q scans was 30% (104 of 345), but within this group patients with high clinical likelihood had a much higher prevalence of 66% (27 of 41) compared to those with low clinical likelihood (16% [11 of 68]) (6) (Fig 10).

The interpretation criteria provided in Tables 3 and 4 are to be regarded as guidelines, not absolute rules to be followed. These criteria are simply not detailed enough to optimize V/Q scan interpretation, which is why the gestalt method used by experienced readers works the best. If one

Table 4: PISAPED Criteria

Interpretation	Imaging Findings*
Normal	No perfusion defects of any kind
Near normal	Perfusion defects smaller or equal in size and shape to the following CXR abnormalities: cardiomegaly; enlarged aorta, hila, and mediastinum; elevated diaphragm; blunting of costophrenic angle; pleural thickening; intrafissural collection of liquid
Abnormal (PE positive)	Single or multiple wedge-shaped perfusion defects with or without matching CXR abnormalities; wedge-shaped areas of overperfusion usually coexist
Abnormal (PE negative)	Single or multiple perfusion defects other than wedge shaped, with or without matching CXR abnormalities; wedge-shaped areas of overperfusion usually not seen

*CXR = chest radiography.

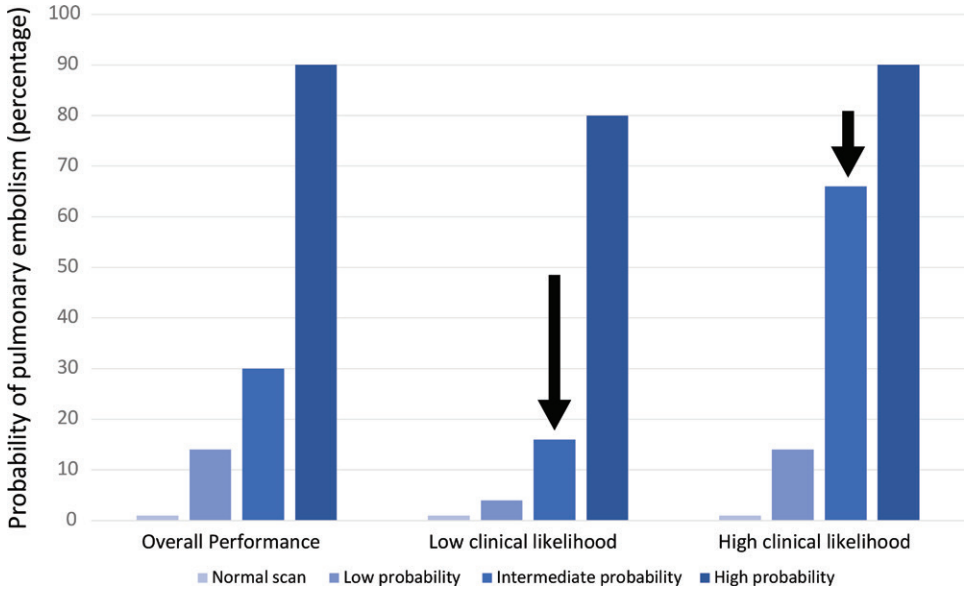

Figure 10. Importance of pretest probability. For intermediate-probability V/Q scan, the presence of PE is highly variable according to the pretest probability, ranging from 16% in patients with low clinical likelihood (long arrow) to 66% in patients with high clinical likelihood (short arrow).

reads the PIOPED interpretation criteria, they contain the words "segmental perfusion defect." Except for the size of the defect, no information is provided about other important characteristics, such as its severity (absent perfusion, markedly decreased perfusion, decreased perfusion, mildly decreased perfusion), the level of confidence in its shape (definitely segmental, likely segmental, possibly segmental), the randomness of the defects, and so on.

An obvious major problem with the PIOPED criteria is that if there are multiple perfusion defects that are judged to be small (24% of a segment), the recommended interpretation is low probability for PE. If a second observer thinks the defects are 26% of a segment (moderate size), the recommended interpretation is high probability! In addition, several pathologic conditions are known to cause perfusion defects with smaller or no corresponding ventilation defects (eg, pulmonary vasculitis, tumor emboli, pulmonary fibrosis, fibrosing mediastinitis) (38–41). Accounting for this clinical information is important in the gestalt method but ignored with the PIOPED criteria.

A seasoned nuclear medicine physician can provide an accurate interpretation by combining clinical data and ancillary findings with their clinical knowledge—rather than by rigidly adhering to interpretation criteria—to achieve a gestalt interpretation, with an area under the curve (AUC) of 0.95–0.98 (3). Many advocate this approach, but it is not always possible to have an experienced nuclear medicine physician immediately available.

SPECT offers increased contrast resolution, and hybrid imaging with SPECT/CT results in greater sensitivity and specificity, as well as a marked reduction in nondiagnostic studies (42). Trinary systems (PE present, PE absent,

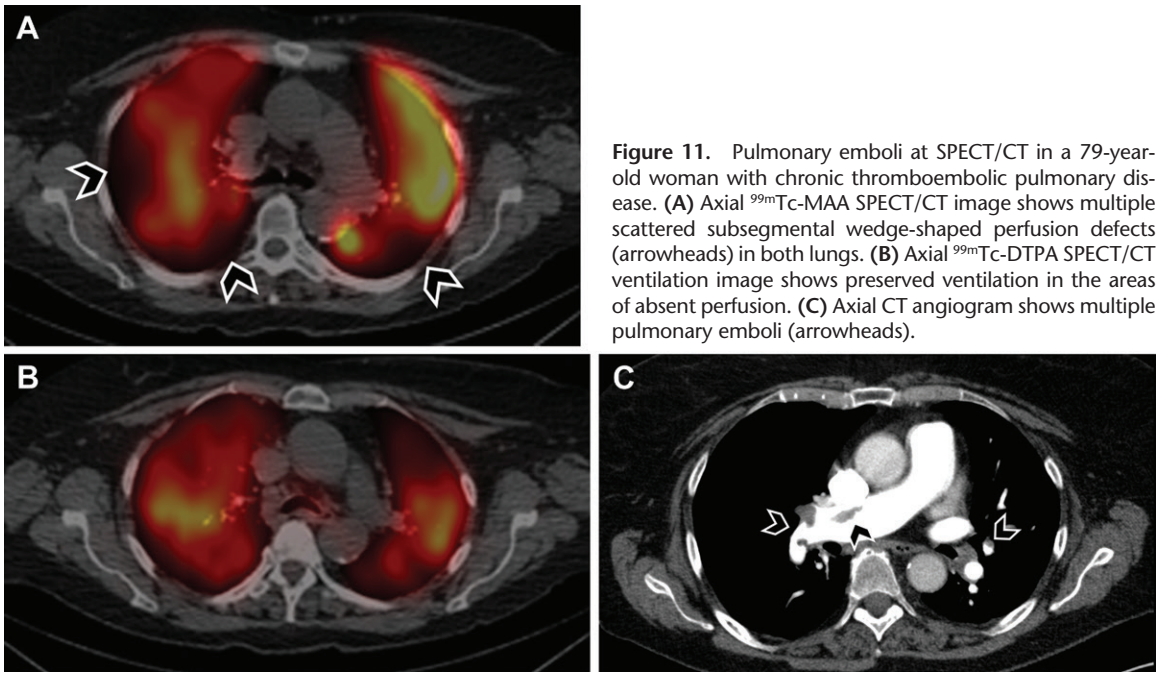

Figure 11. Pulmonary emboli at SPECT/CT in a 79-year-old woman with chronic thromboembolic pulmonary disease. **(A)** Axial ^{99m}Tc-MAA SPECT/CT image shows multiple scattered subsegmental wedge-shaped perfusion defects (arrowheads) in both lungs. **(B)** Axial ^{99m}Tc-DTPA SPECT/CT ventilation image shows preserved ventilation in the areas of absent perfusion. **(C)** Axial CT angiogram shows multiple pulmonary emboli (arrowheads).

Table 5: V/Q SPECT Diagnosis of PE per 2019 EANM Guidelines

Interpretation	Imaging Findings
PE present	V/P mismatch of ≥one segment or two subsegments in keeping with pulmonary vascular anatomy (wedge-shaped defects with base projecting to lung periphery)
PE absent	Normal perfusion Matched or reversed-mismatched V/P defects of any size, shape, or number in absence of mismatch Mismatch that does not follow lobar, segmental, or subsegmental pattern
Nondiagnostic for PE	Widespread V/P abnormalities not typical of specific diseases

or nondiagnostic study) are more accepted in interpretation of V/Q SPECT studies and may also be applied in planar V/Q imaging (42). Per the 2019 EANM guidelines, a V/Q SPECT study is interpreted as positive for PE when there are one or more segmental mismatches or two subsegmental mismatches (43) (Fig 11). SPECT/CT interpretation criteria generally follow EANM guidelines and are summarized in Table 5 (43).

V/Q Scan versus CTPA

Whereas pulmonary angiography has historically been the standard of reference for diagnosis of PE, CTPA is now considered the most sensitive method of evaluating for acute PE (44). In the PIOPED II study, Wittram et al (45) showed that when pulmonary angiography and CTPA results were discordant, the pulmonary angiography result was more likely to be falsely abnormal. CTPA offers many advantages, as it is faster to perform, readily available, easier to interpret, and can provide alternative explanations for the patient's symptoms in cases where PE is not identified. In the setting of PE, CT can demonstrate findings of right heart strain (Fig 12).

The accuracy of CTPA comes at the cost of increased exposure to ionizing radiation, especially to the breasts and lungs, although fetal radiation exposure in pregnant patients remains well below safety levels and is probably comparable for both studies (46,47). The calculated lifetime relative risk of radiation-induced breast or lung cancer in a 25-year-old woman after a single CTPA examination is reported to be 1.011 and 1.022, respectively (48).

Even though CTPA—rather than a lung scan—is considered the current reference standard for diagnosing acute PE (49), Anderson et al (44) showed that diagnostic algorithms using either CTPA or V/Q scan have proved to be comparably safe for excluding the diagnosis of PE.

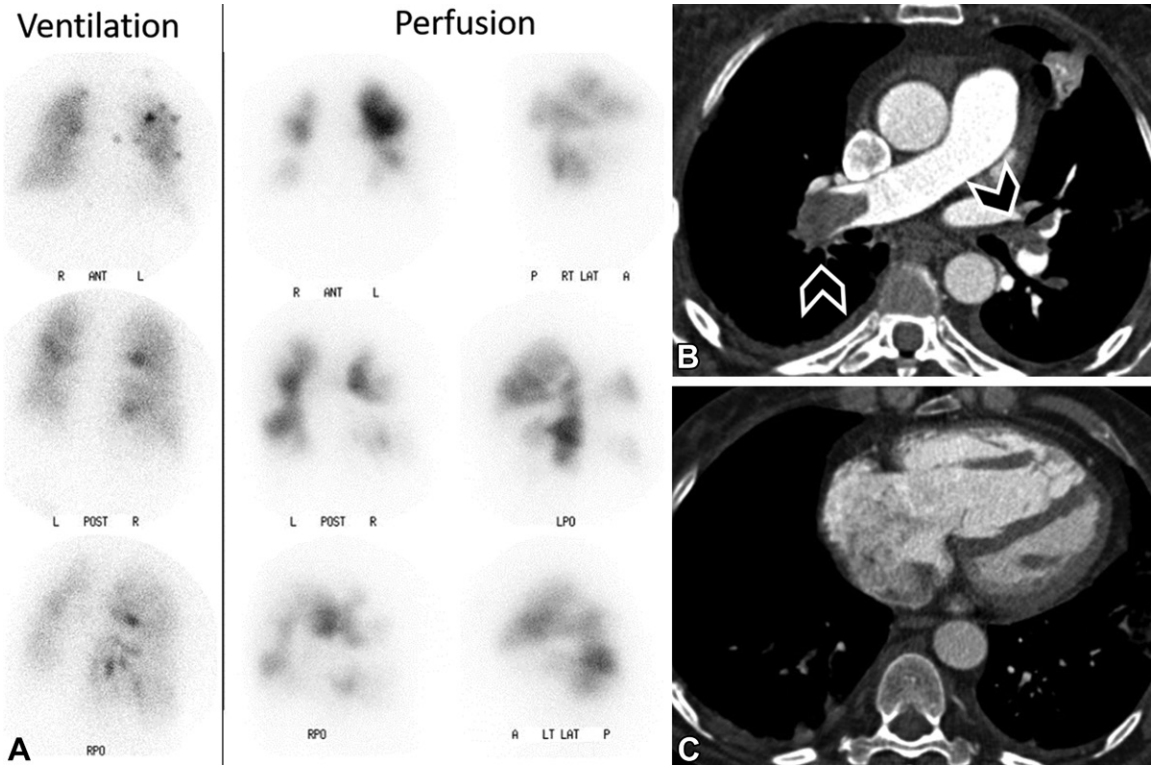

Figure 12. Advantage of CT over V/Q scan in a 51-year-old woman with shortness of breath, fatigue, and lower extremity edema. **(A)** Images from V/Q scan show extensive bilateral pulmonary emboli. Throughout the figures, *A* = anterior, *L* = left, *LT LAT* = left lateral, *P* = posterior, *R* = right, *RT LAT* = right lateral. **(B)** Axial CT image obtained 3 hours after the V/Q scan shows extensive bilateral pulmonary emboli (arrowheads). **(C)** Axial CT image also shows severe right ventricular strain, with right ventricular dilatation and septal bowing to the left.

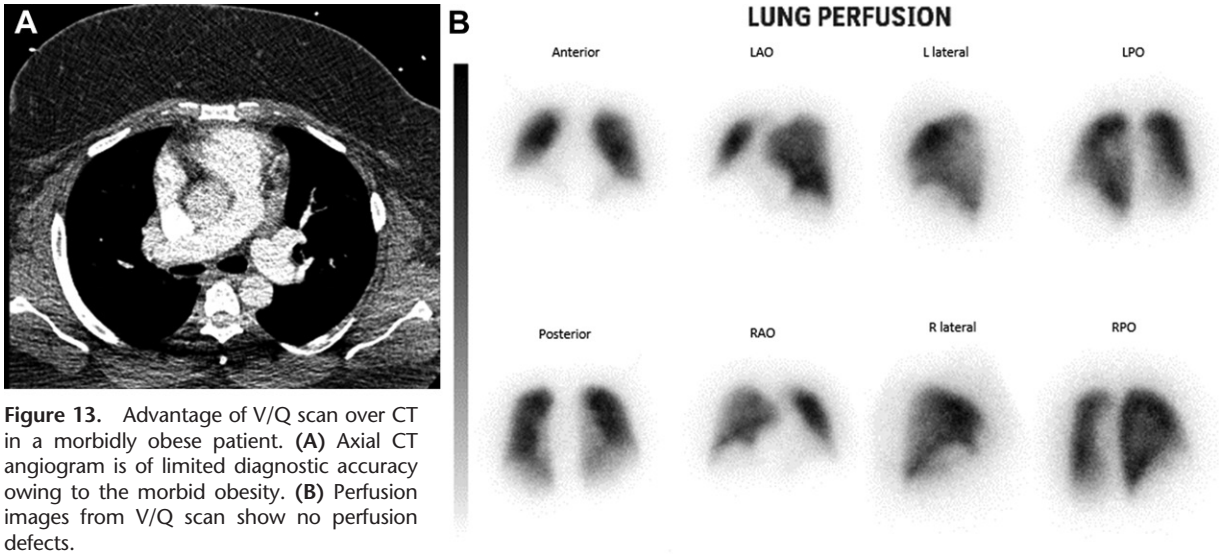

Figure 13. Advantage of V/Q scan over CT in a morbidly obese patient. **(A)** Axial CT angiogram is of limited diagnostic accuracy owing to the morbid obesity. **(B)** Perfusion images from V/Q scan show no perfusion defects.

Even though the detection rate of PE is higher with CTPA, Anderson et al (50) also suggested that some of the diagnosed cases represent clinically unimportant disease. The clinical relevance of small pulmonary emboli detected at CTPA and the question of overdiagnosis and overtreatment remain a hot topic, which is too expansive to be discussed here (51).

In clinical practice, the main advantages of V/Q scan over CTPA are the ability of V/Q scan to provide physiologic information (eg, clot burden, relative flow, reverse mismatch), the portability of the planar V/Q study, and the lack of iodinated contrast material, which makes V/Q scan safe to perform in patients with allergies or altered renal function. V/Q scan can also be performed in mor-

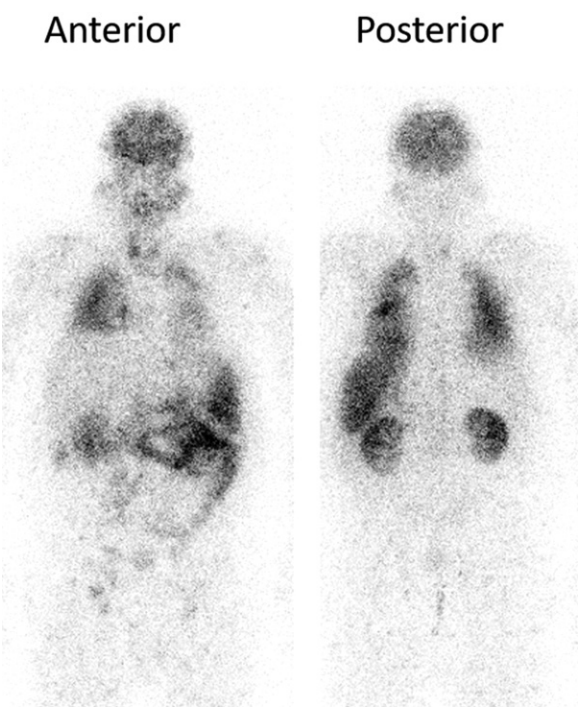

Figure 14. Anatomic right-to-left shunt after Blalock-Taussig shunt, modified Fontan procedure, and revised fenestrated Fontan procedure in a 32-year-old man with a history of pulmonary atresia. Besides tracer deposition in the lungs, there is deposition in the systemic circulation (brain, kidneys, thyroid gland, spleen, soft tissues), consistent with a large right-to-left shunt. After intravenous tracer injection into the right forearm, 19% of blood flow went to the lungs while 81% went to the systemic circulation. Activity in the thyroid gland could be due to shunting, as in this case, or to radiotracer dissociation (free pertechnetate). Right-to-left shunt is quantified as systemic counts (total body counts – lung counts) divided by total body counts.

bidly obese patients, where CT can be limited by artifacts or when the patient weight is above the limit for the CT table (Fig 13). Even with newer techniques, the effective radiation dose of CT is often higher than that of V/Q scan (52).

Within the limits of heterogeneous data and lack of prospective studies, the sensitivity and specificity of V/Q SPECT in detection of PE are comparable to those of CTPA (42). However, lung scan is more appropriate than CTPA for detecting chronic thromboembolic pulmonary disease as a cause of pulmonary hypertension (25,53,54). The American College of Cardiology Working Group recommends V/Q scan in all patients with unexplained pulmonary hypertension, primarily to assess for chronic thromboembolic pulmonary hypertension (CTEPH) (55). V/Q scan demonstrated sensitivity of 90%–100% and specificity of 94%–100% for differentiation between idiopathic pulmonary arterial hypertension (IPAH) and CTEPH (25). Underdiagnosis of chronic PE is compounded by the infrequent use of lung V/Q scan, despite guideline recommendations (56).

Quantitative Lung Scintigraphy

Quantitative lung scintigraphy is a valuable clinical tool for determining the contribution of each lung or a specific anatomic area to overall pulmonary function. Additional less popular uses include established and emerging applications, such as predicting posttreatment pulmonary function before lung cancer resection or radiation therapy and evaluating for bronchiolitis obliterans after lung transplant. ^{99m}Tc-MAA is appropriate for the perfusion scan, and ^{133}Xe or Technegas is preferable for the ventilation scan to avoid central deposition of aerosolized liquids (57). With its washout phase, xenon allows better evaluation of COPD, which may complicate the postoperative period.

Congenital Heart Disease

Congenital heart disease (CHD) encompasses a wide range of cardiovascular anomalies, which could be evaluated with different imaging modalities. Quantitative lung scintigraphy remains critical for its ability to provide physiologic functional information. Asymmetric pulmonary perfusion is a predictor of outcome and exercise capacity in patients with complex CHD and is the most common anomaly seen in CHD (58) (Fig E7). Quantitative measurements allow accurate estimation and can be performed for differential lung function, zone function (upper, mid, and lower lung zones), or lobar function if SPECT/CT is performed.

Right-to-Left Shunt

Right-to-left shunt (Fig 14) is seen with CHD—including septal defects—and noncardiac causes, such as pulmonary arteriovenous malformation in hereditary hemorrhagic telangiectasia, and hepatopulmonary syndrome. A perfusion scan with whole-body images has the unique ability to quantify the degree of shunting by comparing the counts in a region of interest drawn over the lungs to the counts in a region of interest drawn over the remainder of the body. In right-to-left shunt, blood flow bypasses the pulmonary circulation and goes directly to the systemic circulation in the brain, kidneys, and other organs. In cases where right-to-left shunt is not clinically known or suspected but renal activity is seen on ^{99m}Tc-MAA images, dedicated images of the brain can be obtained to confirm right-to-left shunt as a cause of renal deposition rather than free technetium, which also deposits in the thyroid gland, salivary glands, and stomach (59) (Fig 15).

Pretreatment Planning for Lung Cancer

Quantitative lung scintigraphy is considered the standard of reference for estimating the expected remaining pulmonary function after partial or total lung resection for lung cancer (60). V/Q

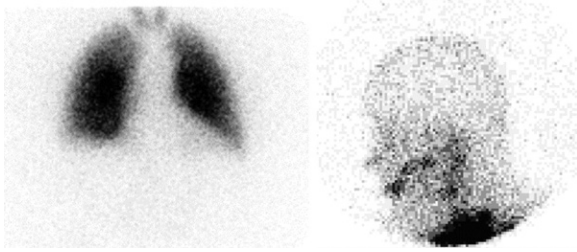

Figure 15. Free pertechnetate in a 43-year-old woman evaluated for pulmonary hypertension. Left: Anterior ^{99m}Tc-MAA perfusion image shows thyroid uptake along the most superior aspect of the lungs. Investigation revealed that the perfusion scintigraphy was delayed for approximately 2 hours after the radiopharmaceutical was drawn into the syringe. Oxygen within the syringe likely oxidized the reduced ^{99m}Tc, which may have dissociated from the MAA during the delay, resulting in free pertechnetate. Right: Additional lateral view of the head shows uptake in the salivary glands but not in the brain, ruling out an anatomic right-to-left shunt.

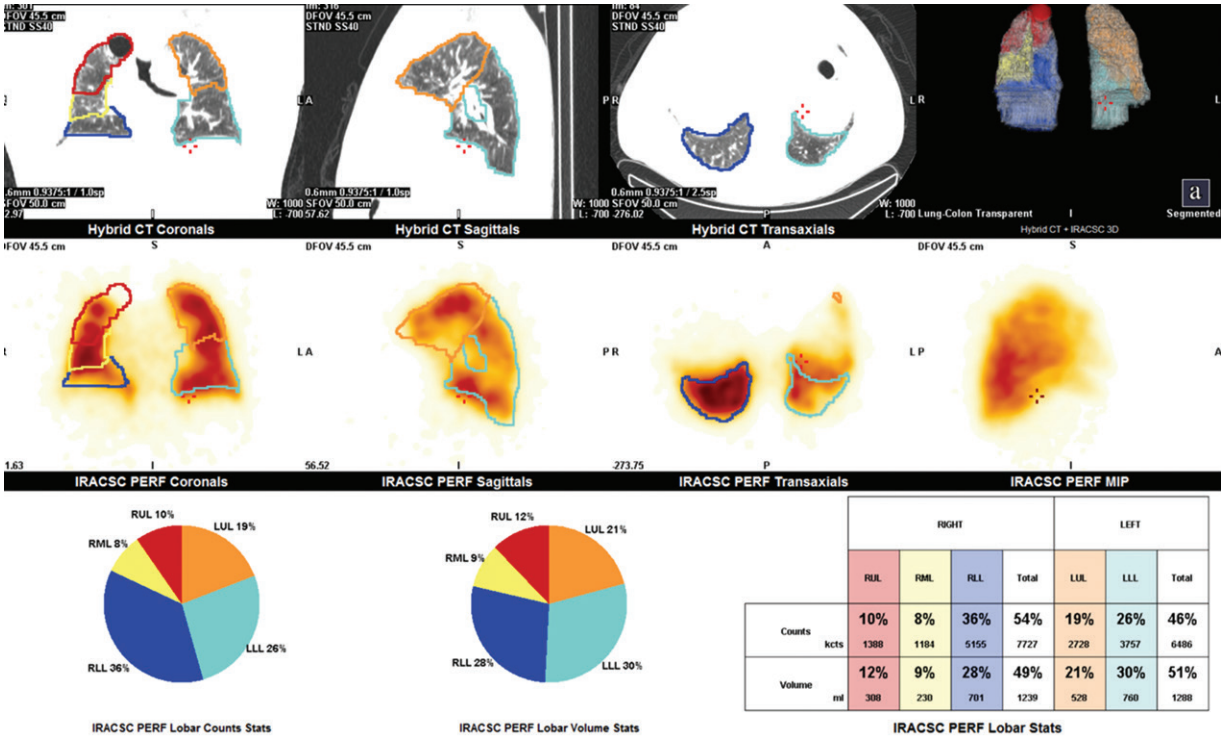

Figure 16. Perfusion SPECT/CT for pretreatment workup of lung cancer in a 60-year-old man with right upper lobe *(RUL)* squamous cell carcinoma. Perfusion SPECT/CT allows quantification of the pulmonary perfusion of each specific lobe, to determine the expected residual lung function after resection of a specific lobe or lobes. *LLL* = left lower lobe, *LUL* = left upper lobe, *RLL* = right lower lobe, *RML* = right middle lobe.

SPECT is also used to optimize planning of radiation fields for lung cancer, to avoid the most functional zones in the lungs (61). Quantitative lung scintigraphy is used to estimate the expected postoperative or post–radiation therapy forced expiratory volume in 1 second (FEV_1) on the basis of the contribution of each lung zone (at planar imaging) or lobe (at SPECT); patients should have an expected FEV_1 of greater than 1 L postoperatively and greater than 0.8 L after radiation therapy (61) (Fig 16).

Presurgical Planning for Lung Volume Reduction Surgery

To improve the symptoms and quality of life in patients with COPD, such as emphysema from smoking or α_1-antitrypsin deficiency, lung volume reduction surgery is performed to resect the less functional portions of the lungs (62) and allow improved respiratory mechanics of the spared lung. This is most helpful in cases where distribution of the emphysema is heterogeneous or atypical (63) (Fig 17).

Before Lung Transplant

In cases of bilateral lung transplant, the less functional lung will be resected first to avoid cardiac bypass during the procedure (64). A pitfall in imaging pretransplant patients is that confluent areas of parenchymal disease, specifically fibrosis, result in large perfusion defects; these mismatched defects are often misinterpreted as high probability for PE by nonexperienced readers (64) (Fig 18).

After Lung Transplant

Bronchiolitis obliterans, the main cause of chronic lung allograft dysfunction, occurs in 50% of transplants at 5 years and 90% at 15 years (65,66). Even though high-resolution CT is critical in evaluation, lung scintigraphy can demonstrate early

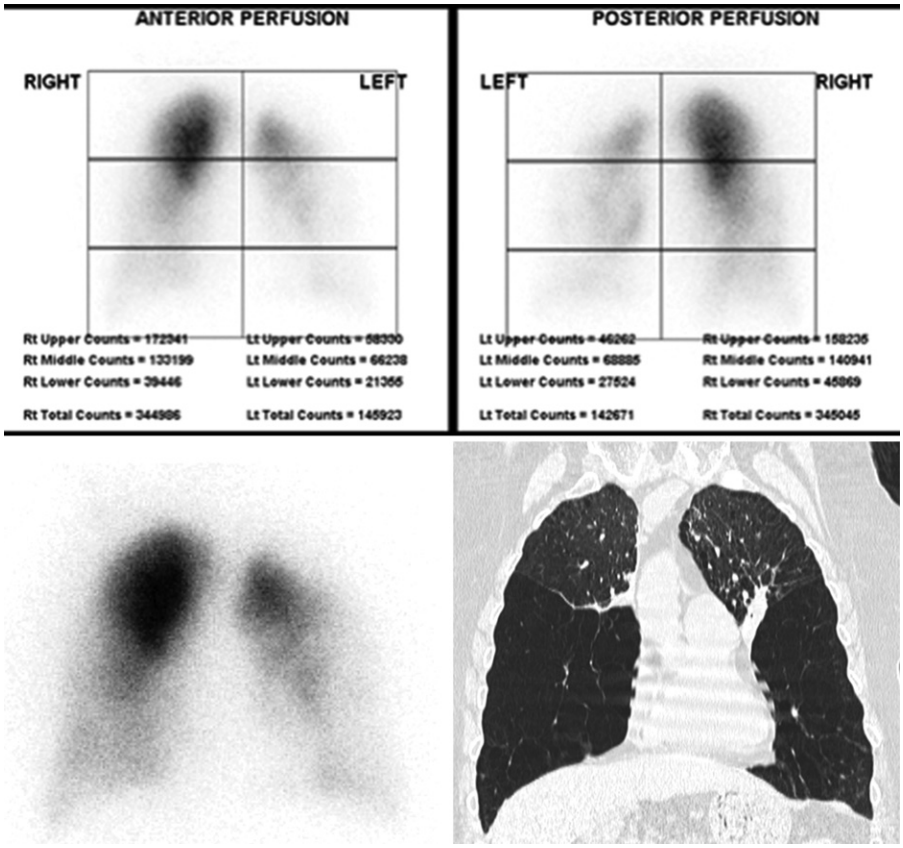

Figure 17. Presurgical evaluation with perfusion scan in a 62-year-old woman presenting for lung volume reduction surgery. Perfusion images and coronal CT image (bottom right) show atypical distribution of emphysema, with lower lobe predominance due to α_1-antitrypsin deficiency. Quantification is performed by calculating the geometric mean of counts in the anterior and posterior projections (square root of the multiplication product).

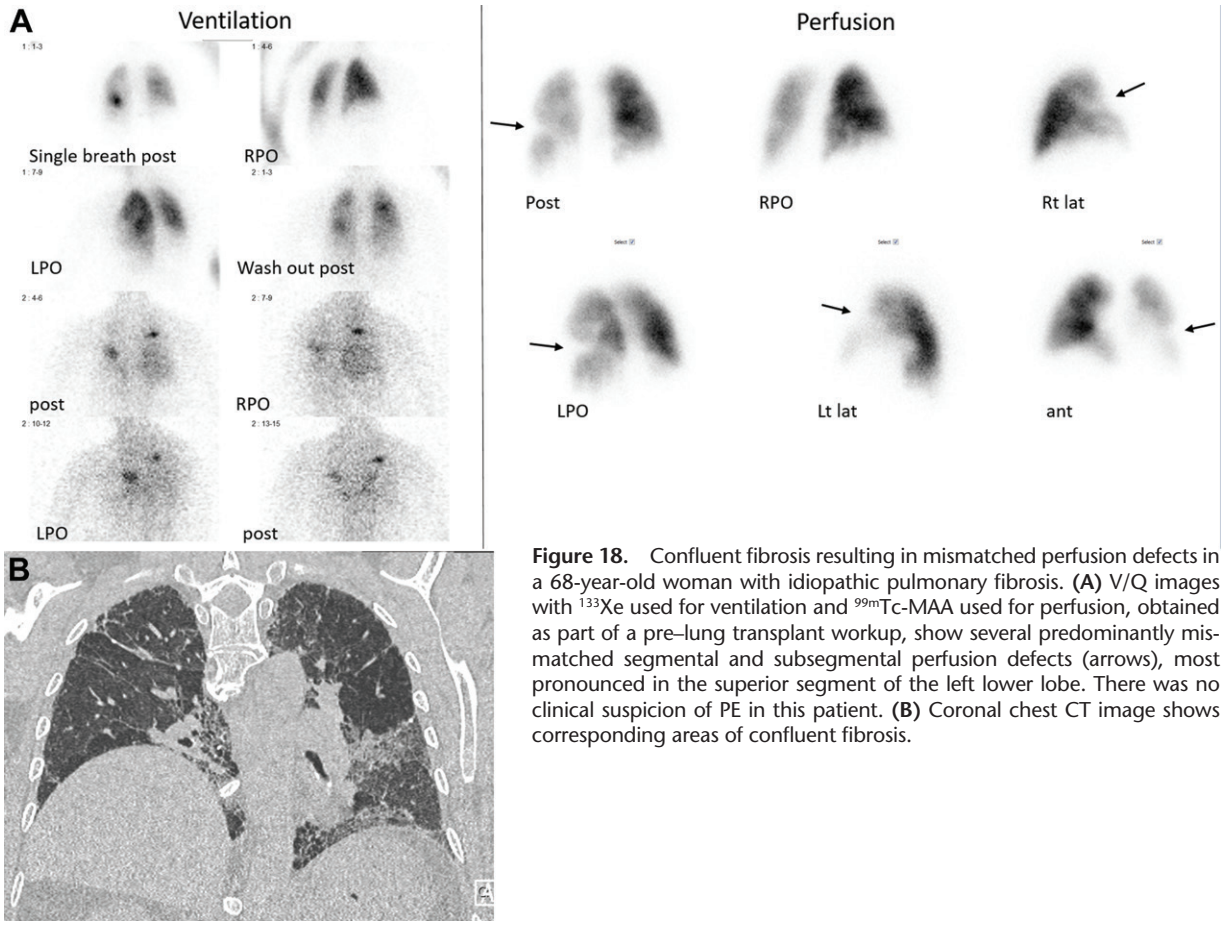

Figure 18. Confluent fibrosis resulting in mismatched perfusion defects in a 68-year-old woman with idiopathic pulmonary fibrosis. **(A)** V/Q images with ^{133}Xe used for ventilation and ^{99m}Tc-MAA used for perfusion, obtained as part of a pre–lung transplant workup, show several predominantly mismatched segmental and subsegmental perfusion defects (arrows), most pronounced in the superior segment of the left lower lobe. There was no clinical suspicion of PE in this patient. **(B)** Coronal chest CT image shows corresponding areas of confluent fibrosis.

Figure 19. Chronic lung allograft dysfunction in an 18-year-old woman with worsening pulmonary function after bilateral lung transplant 3 years earlier. **(A)** ^{133}Xe ventilation images show patchy areas of decreased ventilation, worst in the left upper lobe, with several areas of marked xenon retention, greater on the left than on the right. The perfusion images show essentially matched patchy decreased perfusion, most severe in the left lung, consistent with bronchiolitis obliterans or chronic rejection, subsequently confirmed with lung biopsy results. The hot spot corresponds to the site of injection in the chest port. **(B)** Axial CT images show mosaic attenuation in the upper lung zones predominantly and diffuse areas of air trapping bilaterally with associated bronchiectasis bilaterally, involving the upper and lower lobes.

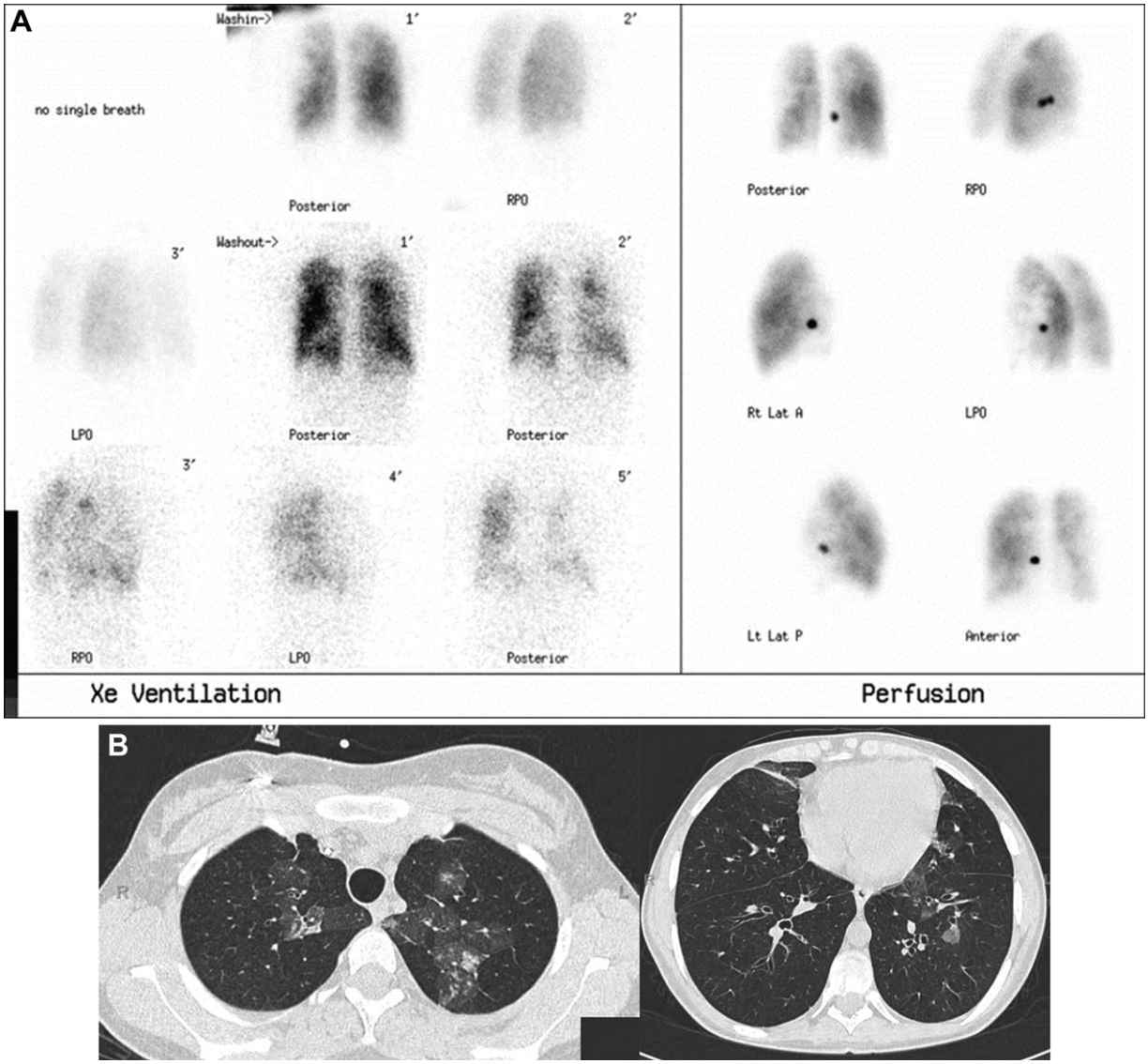

functional changes before any detectable anatomic anomaly; nevertheless, functional evaluation with daily spirometry can demonstrate changes before scintigraphy. Bronchiolitis obliterans has an obstructive pattern on xenon ventilation scans (Fig 19). Bronchial stenosis is another common complication after lung transplant, occurring in 4%–24% of patients; a lung scan can demonstrate the areas of decreased ventilation (64).

Less Common Pathologic Conditions Detected at Lung Scintigraphy

Pulmonary vasculitis has a variable radiologic appearance, which may include vessel wall thickening, nodular or ground-glass opacities, cavitary lesions, and consolidations (67). Clinical manifestation with hemoptysis and chest pain, as well as scintigraphic findings of multiple segmental mismatched perfusion defects, may overlap in PE and vasculitis (Fig E8). CTPA is helpful for distinguishing between the two entities: PE shows intravascular filling defects, whereas vasculitis demonstrates vessel wall abnormalities rather than intraluminal abnormalities (38).

Tumor microemboli, most commonly from gastric or breast cancer (68), and lymphangitic spread, from breast, lung, or gastrointestinal primaries (69), can mimic PE at clinical presentation. Furthermore, mismatched wedge-shaped

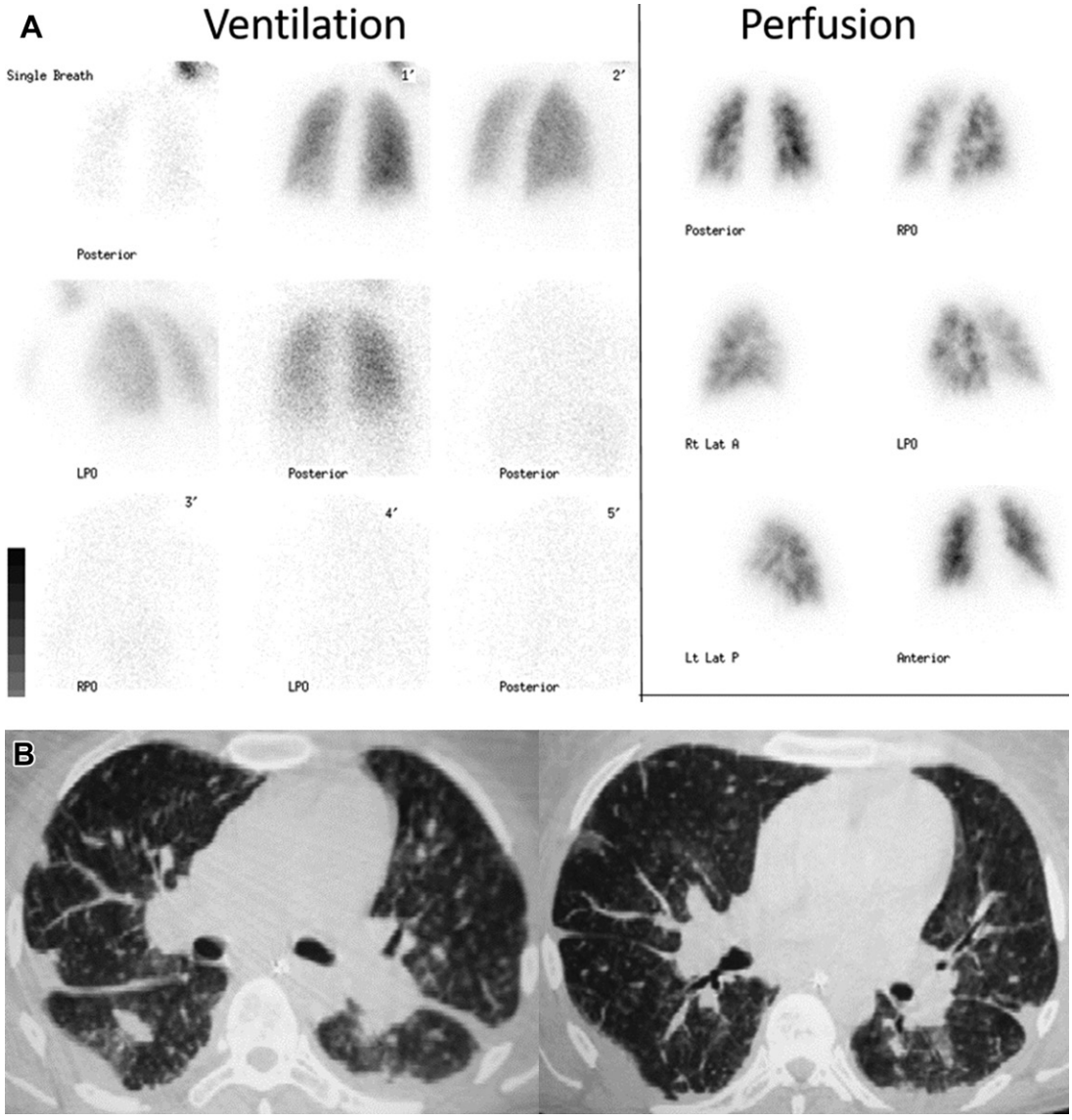

Figure 20. Lymphangitic carcinomatosis in a 41-year-old woman with metastatic cervical carcinoma who presented with severe dyspnea. **(A)** Images from V/Q scan show normal ^{133}Xe ventilation and diffuse small mismatched perfusion defects, resulting in the segmental contouring sign or contour mapping appearance. **(B)** Axial chest CT images show no evidence of PE. However, nodular thickening of many of the interlobar septa is present, suggestive of lymphangitic spread of carcinoma.

perfusion defects can be seen, resulting in a V/Q scan appearance typical of high probability for PE. However, the segmental defects in tumor microemboli are smaller, more numerous, more peripheral, bilateral, and homogeneously spread throughout the periphery of the lungs, outlining the bronchopulmonary segments and resulting in a contour mapping appearance (39). In general, chest radiographs are normal, and the emboli can improve with treatment of the underlying neoplasm. Lymphangitic spread has been described as a consequence of these tumor microemboli, with invasion of the interstitium and lymphatic vessels (Fig 20) (70).

Superior vena cava obstruction can cause shunting of blood from the systemic veins to the portal system, mainly through the internal mammary vein to the paraumbilical vein, then to the left portal vein to deposit primarily in segment IV, resulting in the quadrate sign, or what was initially described as the hot spot sign on ^{99m}Tc–sulfur colloid images (71); it can also be seen at contrast-enhanced CT. On lung perfusion images, intravenously administered MAA will follow this route, showing increased uptake in the anterior abdominal wall and left hepatic lobe (Fig 21) (72).

Acute respiratory distress syndrome (ARDS) is acute respiratory failure characterized by diffuse alveolar capillary and epithelial damage, resulting in extensive pulmonary edema and severe hypoxemia. There is diffuse endothelial injury

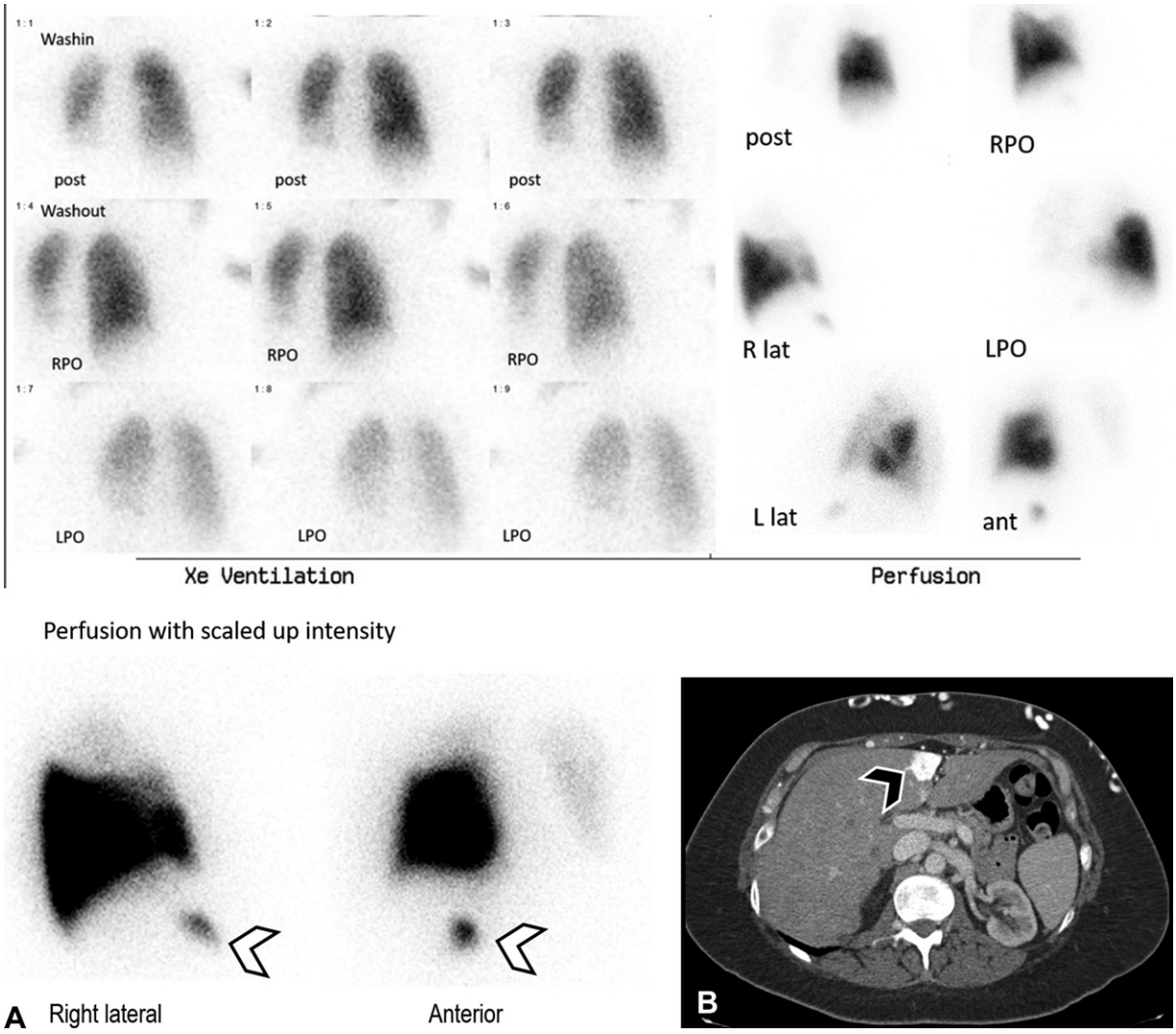

Figure 21. Superior vena cava obstruction in a 43-year-old woman with fibrosing mediastinitis. **(A)** Images from V/Q scintigraphy show absent perfusion of the left lung and right upper lobe and decreased perfusion of the right middle lobe—with better ^{133}Xe ventilation—secondary to multivessel occlusion caused by fibrosing mediastinitis. There is focal increased activity (arrowheads) in the medial left hepatic lobe, segment IV, corresponding to the focal hepatic hot spot sign traditionally described at sulfur colloid imaging. **(B)** Axial CT image shows marked enhancement of the same area in hepatic segment IV (arrowhead) and extensive body wall venous collaterals.

with associated macro- and microthrombi, which can progress to fibrocellular intimal proliferation that can obliterate small vessels, causing pulmonary hypertension. The appearance at lung scintigraphy can be variable, because areas can have alternatively low or high ventilation-perfusion ratio. Multiple bilateral mismatched defects have been described (73).

Air leak, which can result from central bronchopleural fistula or more peripheral alveolopleural fistula, is a serious complication of many diseases and surgical procedures and is challenging to localize at imaging (74). Ventilation scintigraphy can show tracer leakage into the pleural space at the site of fistula (75). The perfusion scan would show absent uptake in the corresponding location, or decreased uptake in cases where perfusion imaging is performed with residual activity from the ventilation scan (Fig 22).

An additional variety of pathologic conditions in the chest and upper abdomen can be incidentally noted at V/Q scan (Fig 23).

Conclusion

V/Q scan has been used for many years and is helpful in investigation of several diseases. This review summarizes the basics of lung scintigraphy; describes its indications and interpretation guidelines, especially for PE; elaborates on the less commonly known applications of quantitative V/Q scan; and presents an image-rich display of a wide range of abnormalities and their scintigraphic appearances. This will help residents

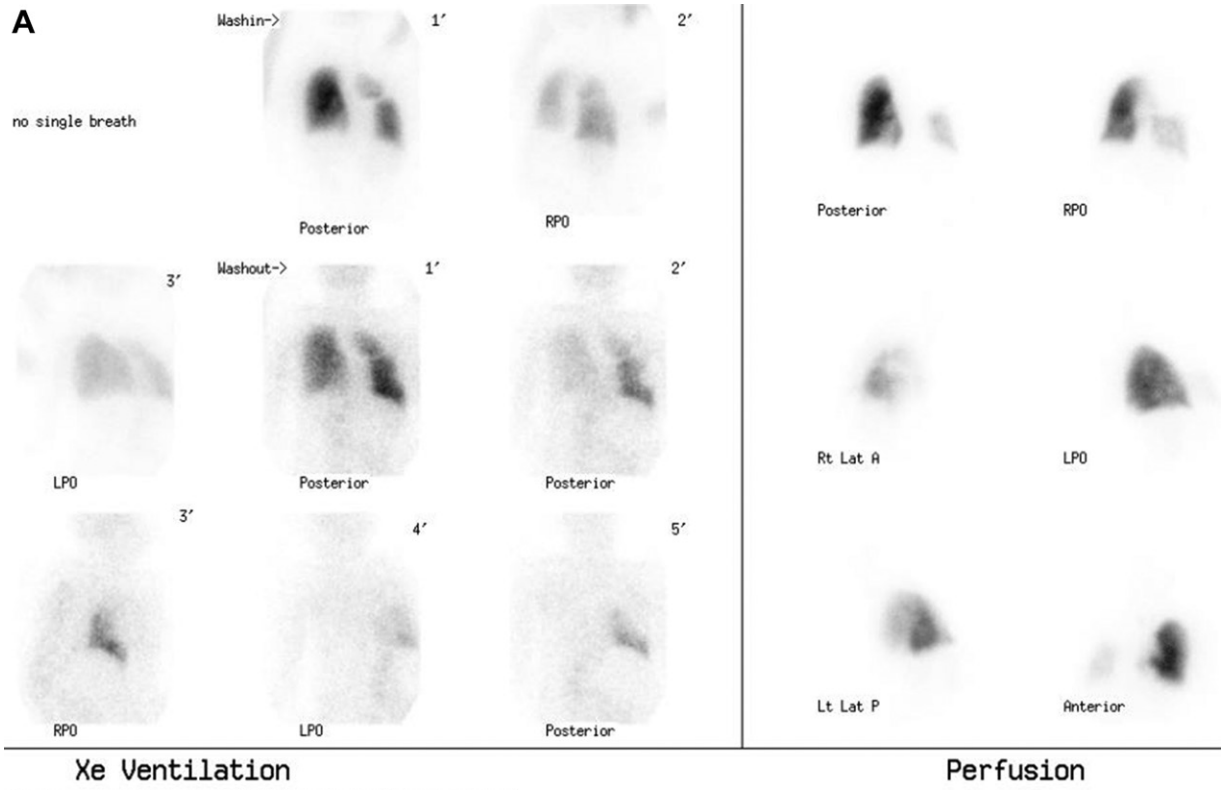

Figure 22. Bronchopleural fistula in a 50-year-old woman after right lower lobectomy for right lung cancer. **(A)** Images from V/Q scan show xenon accumulation in the right upper hemithorax with absent perfusion. **(B)** Axial CT image shows a cavity in the right upper hemithorax with a bronchopleural fistula (arrowhead), which allowed the xenon to reach the loculated pneumothorax.

better interpret V/Q scans and understand the potential scope of this study and its role in patient management.

References

1. Quinn JL 3rd, Whitley JE, Hudspeth AS, Prichard RW. Early Clinical Applications of Lung Scintiscanning. Radiology 1964;82(2):315–317.
2. Sinner WN. Computed tomographic patterns of pulmonary thromboembolism and infarction. J Comput Assist Tomogr 1978;2(4):395–399.
3. Hagen PJ, Hartmann IJ, Hoekstra OS, Stokkel MP, Teule GJ, Prins MH. How to use a gestalt interpretation for ventilation-perfusion lung scintigraphy. J Nucl Med 2002;43(10):1317–1323.
4. McNeil BJ. Ventilation-perfusion studies and the diagnosis of pulmonary embolism: concise communication. J Nucl Med 1980;21(4):319–323.
5. Biello DR. Radiological (scintigraphic) evaluation of patients with suspected pulmonary thromboembolism. JAMA 1987;257(23):3257–3259.
6. PIOPED Investigators. Value of the ventilation/perfusion scan in acute pulmonary embolism: results of the Prospective Investigation of Pulmonary Embolism Diagnosis (PIOPED). JAMA 1990;263(20):2753–2759.
7. Gottschalk A, Stein PD, Goodman LR, Sostman HD. Overview of Prospective Investigation of Pulmonary Embolism Diagnosis II. Semin Nucl Med 2002;32(3):173–182.
8. Miniati M, Pistolesi M, Marini C, et al. Value of perfusion lung scan in the diagnosis of pulmonary embolism: results of the Prospective Investigative Study of Acute Pulmonary Embolism Diagnosis (PISA-PED). Am J Respir Crit Care Med 1996;154(5):1387–1393.
9. Bajc M, Neilly JB, Miniati M, et al. EANM guidelines for ventilation/perfusion scintigraphy. I. Pulmonary imaging with ventilation/perfusion single photon emission tomography. Eur J Nucl Med Mol Imaging 2009;36(8):1356–1370.
10. Watanabe N, Fettich J, Küçük NÖ, et al. Modified PISAPED Criteria in Combination with Ventilation Scintigraphic Finding for Predicting Acute Pulmonary Embolism. World J Nucl Med 2015;14(3):178–183.
11. COVID-19 and Ventilation/Perfusion (V/Q) Lung Studies. J Nucl Med 2020;61(10):23N–24N.
12. COVID-19: ACR Statement on Nuclear Medicine Ventilation Scans. American College of Radiology. https://www.acr.org/Advocacy-and-Economics/ACR-Position-Statements/COVID19-Nuclear-Medicine-Ventilation-Scans. Updated March 25, 2020. Accessed February 2, 2021.
13. Magnant J, Vecellio L, de Monte M, et al. Comparative analysis of different scintigraphic approaches to assess pulmonary ventilation. J Aerosol Med 2006;19(2):148–159.
14. Lloyd JJ, Shields RA, Taylor CJ, Lawson RS, James JM, Testra HJ. Technegas and Pertechnegas particle size distribution. Eur J Nucl Med 1995;22(5):473–476.
15. Parker JA, Coleman RE, Grady E, et al. SNM practice guideline for lung scintigraphy 4.0. J Nucl Med Technol 2012;40(1):57–65.
16. Smart RC, Lyons NR, Burke JJ, Wood CF. A combined procedure for 99mTc aerosol ventilation and perfusion imaging. Eur J Nucl Med 1985;11(2-3):65–68.

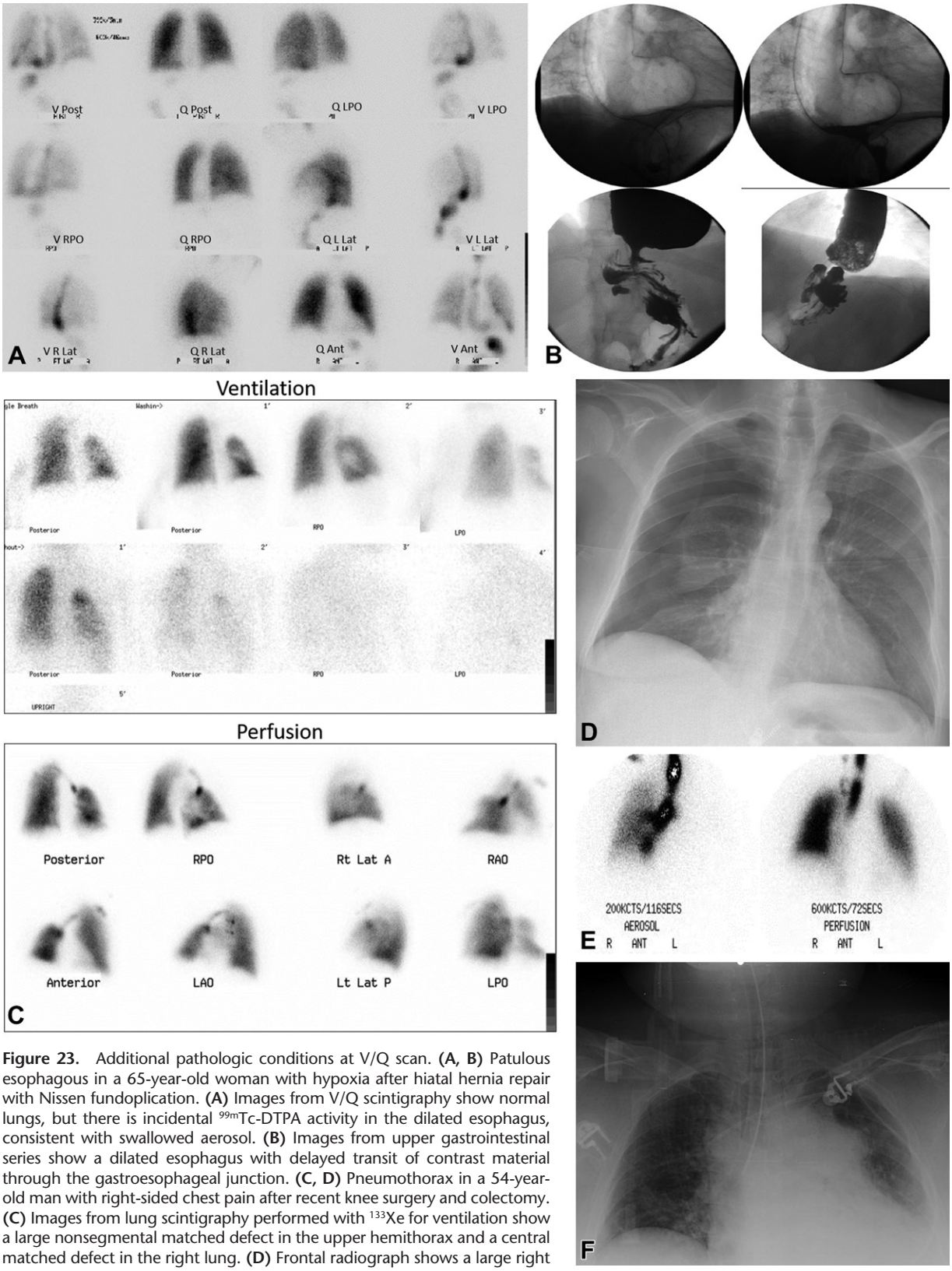

Figure 23. Additional pathologic conditions at V/Q scan. **(A, B)** Patulous esophagous in a 65-year-old woman with hypoxia after hiatal hernia repair with Nissen fundoplication. **(A)** Images from V/Q scintigraphy show normal lungs, but there is incidental ^{99m}Tc-DTPA activity in the dilated esophagus, consistent with swallowed aerosol. **(B)** Images from upper gastrointestinal series show a dilated esophagus with delayed transit of contrast material through the gastroesophageal junction. **(C, D)** Pneumothorax in a 54-year-old man with right-sided chest pain after recent knee surgery and colectomy. **(C)** Images from lung scintigraphy performed with ^{133}Xe for ventilation show a large nonsegmental matched defect in the upper hemithorax and a central matched defect in the right lung. **(D)** Frontal radiograph shows a large right pneumothorax with collapse of the right lung. **(E, F)** Selective bronchial intubation in a 55-year-old woman found to have pulseless electrical activity after a recent surgical procedure for a right tibial plateau fracture. She had persistent hypoxia despite resuscitation and intubation. **(E)** Ventilation image from lung scintigraphy (left) shows no ^{99m}Tc-DTPA aerosol ventilation of the left lung, which remains well perfused (right). **(F)** Chest radiograph obtained before the V/Q scan shows intubation of the right main-stem bronchus; an attempt to correct this before the lung scan (with ^{133}Xe for ventilation) was unsuccessful. Chest radiography after the lung scan with repeat adjustment demonstrated good positioning (not shown).

17. Mattsson S, Johansson L, Leide Svegborn S, et al. Radiation Dose to Patients from Radiopharmaceuticals: a Compendium of Current Information Related to Frequently Used Substances. Ann ICRP 2015;44(2 suppl):7–321. [Published corrections appear in Ann ICRP 2019;48(1):96 and Ann ICRP 2019;48(1):97.]
18. Moradi F, Morris TA, Hoh CK. Perfusion Scintigraphy in Diagnosis and Management of Thromboembolic Pulmonary Hypertension. RadioGraphics 2019;39(1):169–185.
19. Ziessman HA, O'Malley JP, Thrall JH, Fahey FH. Chapter 17. Nuclear medicine: the requisites. Philadelphia, Pa: Elsevier Saunders, 2014; 424–439.
20. Lutzker LG, Perez LA. Radioactive embolization from upper-extremity thrombophlebitis. J Nucl Med 1975;16(3):241–242.
21. Lee S, Chaturvedi A. Imaging adults on extracorporeal membrane oxygenation (ECMO). Insights Imaging 2014;5(6):731–742.
22. de Groot MR, Turkstra F, van Marwijk Kooy M, Oostdijk AH, van Beek EJ, Büller HR. Value of chest X-ray combined with perfusion scan versus ventilation/perfusion scan in acute pulmonary embolism. Thromb Haemost 2000;83(3):412–415.
23. Sostman HD, Miniati M, Gottschalk A, Matta F, Stein PD, Pistolesi M. Sensitivity and specificity of perfusion scintigraphy combined with chest radiography for acute pulmonary embolism in PIOPED II. J Nucl Med 2008;49(11):1741–1748.
24. Wang F, Fang W, Lv B, et al. Comparison of lung scintigraphy with multi-slice spiral computed tomography in the diagnosis of pulmonary embolism. Clin Nucl Med 2009;34(7):424–427.
25. Galiè N, Humbert M, Vachiery JL, et al. 2015 ESC/ERS Guidelines for the diagnosis and treatment of pulmonary hypertension: the Joint Task Force for the Diagnosis and Treatment of Pulmonary Hypertension of the European Society of Cardiology (ESC) and the European Respiratory Society (ERS): Endorsed by: Association for European Paediatric and Congenital Cardiology (AEPC), International Society for Heart and Lung Transplantation (ISHLT). Eur Heart J 2016;37(1):67–119.
26. Wilkens H, Konstantinides S, Lang IM, et al. Chronic thromboembolic pulmonary hypertension (CTEPH): updated recommendations from the Cologne Consensus Conference 2018. Int J Cardiol 2018;272S:69–78.
27. Derlin T, Kelting C, Hueper K, et al. Quantitation of Perfused Lung Volume Using Hybrid SPECT/CT Allows Refining the Assessment of Lung Perfusion and Estimating Disease Extent in Chronic Thromboembolic Pulmonary Hypertension. Clin Nucl Med 2018;43(6):e170–e177.
28. Nachand D, Huang S, Bullen J, Heresi GA, Renapurkar RD. Assessment of ventilation-perfusion scans in patients with chronic thromboembolic pulmonary hypertension before and after surgery and correlation with clinical parameters. Clin Imaging 2020;66:147–152.
29. Wells PS, Anderson DR, Rodger M, et al. Excluding pulmonary embolism at the bedside without diagnostic imaging: management of patients with suspected pulmonary embolism presenting to the emergency department by using a simple clinical model and D-dimer. Ann Intern Med 2001;135(2):98–107.
30. Le Gal G, Righini M, Roy PM, et al. Prediction of pulmonary embolism in the emergency department: the revised Geneva score. Ann Intern Med 2006;144(3):165–171.
31. Wells PS, Anderson DR, Rodger M, et al. Derivation of a simple clinical model to categorize patients probability of pulmonary embolism: increasing the models utility with the SimpliRED D-dimer. Thromb Haemost 2000;83(3):416–420.
32. ACR Appropriateness Criteria. Suspected Pulmonary Embolism. American College of Radiology. https://acsearch.acr.org/docs/69404/Narrative/. Updated 2016. Accessed February 4, 2021.
33. Walker CM, Rosado-de-Christenson ML, Martínez-Jiménez S, Kunin JR, Wible BC. Bronchial arteries: anatomy, function, hypertrophy, and anomalies. RadioGraphics 2015;35(1):32–49.
34. Amin F, Kyriakopoulos C. Lung Perfusion Scan. Treasure Island, Fla: StatPearls, 2020.
35. Worsley DF, Kim CK, Alavi A, Palevsky HI. Detailed analysis of patients with matched ventilation-perfusion defects and chest radiographic opacities. J Nucl Med 1993;34(11):1851–1853.
36. Pickhardt PJ, Fischer KC. Unilateral hypoperfusion or absent perfusion on pulmonary scintigraphy: differential diagnosis. AJR Am J Roentgenol 1998;171(1):145–150.
37. Sostman HD, Stein PD, Gottschalk A, Matta F, Hull R, Goodman L. Acute pulmonary embolism: sensitivity and specificity of ventilation-perfusion scintigraphy in PIOPED II study. Radiology 2008;246(3):941–946.
38. Haydar AA, Goldsmith DJ. Pulmonary embolism—or vasculitis? J R Soc Med 2004;97(1):27–28.
39. Sostman HD, Brown M, Toole A, Bobrow S, Gottschalk A. Perfusion scan in pulmonary vascular/lymphangitic carcinomatosis: the segmental contour pattern. AJR Am J Roentgenol 1981;137(5):1072–1074.
40. Strickland NH, Hughes JM, Hart DA, Myers MJ, Lavender JP. Cause of regional ventilation-perfusion mismatching in patients with idiopathic pulmonary fibrosis: a combined CT and scintigraphic study. AJR Am J Roentgenol 1993;161(4):719–725.
41. Rossi SE, McAdams HP, Rosado-de-Christenson ML, Franks TJ, Galvin JR. Fibrosing mediastinitis. RadioGraphics 2001;21(3):737–757.
42. Metter D, Tulchinsky M, Freeman LM. Current Status of Ventilation-Perfusion Scintigraphy for Suspected Pulmonary Embolism. AJR Am J Roentgenol 2017;208(3):489–494.
43. Bajc M, Schümichen C, Grüning T, et al. EANM guideline for ventilation/perfusion single-photon emission computed tomography (SPECT) for diagnosis of pulmonary embolism and beyond. Eur J Nucl Med Mol Imaging 2019;46(12):2429–2451.
44. Anderson DR, Barnes DC. Computerized tomographic pulmonary angiography versus ventilation perfusion lung scanning for the diagnosis of pulmonary embolism. Curr Opin Pulm Med 2009;15(5):425–429.
45. Wittram C, Waltman AC, Shepard JA, Halpern E, Goodman LR. Discordance between CT and angiography in the PIOPED II study. Radiology 2007;244(3):883–889.
46. Leung AN, Bull TM, Jaeschke R, et al. American Thoracic Society documents: an official American Thoracic Society/Society of Thoracic Radiology Clinical Practice Guideline—evaluation of suspected pulmonary embolism in pregnancy. Radiology 2012;262(2):635–646.
47. Tromeur C, van der Pol LM, Le Roux PY, et al. Computed tomography pulmonary angiography versus ventilation-perfusion lung scanning for diagnosing pulmonary embolism during pregnancy: a systematic review and meta-analysis. Haematologica 2019;104(1):176–188.
48. Hurwitz LM, Reiman RE, Yoshizumi TT, et al. Radiation dose from contemporary cardiothoracic multidetector CT protocols with an anthropomorphic female phantom: implications for cancer induction. Radiology 2007;245(3):742–750.
49. Palm V, Rengier F, Rajiah P, Heussel CP, Partovi S. Acute Pulmonary Embolism: Imaging Techniques, Findings, Endovascular Treatment and Differential Diagnoses. Rofo 2020;192(1):38–49.
50. Anderson DR, Kahn SR, Rodger MA, et al. Computed tomographic pulmonary angiography vs ventilation-perfusion lung scanning in patients with suspected pulmonary embolism: a randomized controlled trial. JAMA 2007;298(23):2743–2753.
51. Baumgartner C, Tritschler T. Clinical significance of subsegmental pulmonary embolism: an ongoing controversy. Res Pract Thromb Haemost 2020;5(1):14–16.
52. Schembri GP, Miller AE, Smart R. Radiation dosimetry and safety issues in the investigation of pulmonary embolism. Semin Nucl Med 2010;40(6):442–454.
53. Tunariu N, Gibbs SJ, Win Z, et al. Ventilation-perfusion scintigraphy is more sensitive than multidetector CTPA in detecting chronic thromboembolic pulmonary disease as a treatable cause of pulmonary hypertension. J Nucl Med 2007;48(5):680–684.

54. ACR Appropriateness Criteria. Suspected Pulmonary Hypertension. American College of Radiology. https://acsearch.acr.org/docs/71095/Narrative/. Updated 2016. Accessed February 7, 2021.
55. Hoeper MM, Barberà JA, Channick RN, et al. Diagnosis, assessment, and treatment of non-pulmonary arterial hypertension pulmonary hypertension. J Am Coll Cardiol 2009;54(1 suppl):S85–S96.
56. Tapson VF, Platt DM, Xia F, et al. Monitoring for Pulmonary Hypertension Following Pulmonary Embolism: The INFORM Study. Am J Med 2016;129(9):978–985.e2.
57. MacDonald A, Burrell S. Infrequently performed studies in nuclear medicine: part 2. J Nucl Med Technol 2009;37(1):1–13.
58. Fathala A. Quantitative lung perfusion scintigraphy in patients with congenital heart disease. Heart Views 2010;11(3):109–114.
59. Qutbi M. An Easily Overlooked Cause of High Level of Free Pertechnetate in Lung Perfusion Scintigraphy with ^{99m}Tc-MAA Resulting From Improper Kit Reconstitution. Indian J Nucl Med 2020;35(1):91–92.
60. Wernly JA, DeMeester TR, Kirchner PT, Myerowitz PD, Oxford DE, Golomb HM. Clinical value of quantitative ventilation-perfusion lung scans in the surgical management of bronchogenic carcinoma. J Thorac Cardiovasc Surg 1980;80(4):535–543.
61. Elojeimy S, Cruite I, Bowen S, Zeng J, Vesselle H. Overview of the Novel and Improved Pulmonary Ventilation-Perfusion Imaging Applications in the Era of SPECT/CT. AJR Am J Roentgenol 2016;207(6):1307–1315.
62. Caviezel C, Froehlich T, Schneiter D, et al. Identification of target zones for lung volume reduction surgery using three-dimensional computed tomography rendering. ERJ Open Res 2020;6(3):00305-2020.
63. Martini K, Frauenfelder T. Emphysema and lung volume reduction: the role of radiology. J Thorac Dis 2018;10(suppl 23):S2719–S2731.
64. Pinho DF, Banga A, Torres F, Mathews D. Ventilation perfusion pulmonary scintigraphy in the evaluation of pre- and post-lung transplant patients. Transplant Rev (Orlando) 2019;33(2):107–114.
65. Verleden GM, Glanville AR, Lease ED, et al. Chronic lung allograft dysfunction: definition, diagnostic criteria, and approaches to treatment—a consensus report from the Pulmonary Council of the ISHLT. J Heart Lung Transplant 2019;38(5):493–503.
66. Chambers DC, Zuckermann A, Cherikh WS, et al. The International Thoracic Organ Transplant Registry of the International Society for Heart and Lung Transplantation: 37th adult lung transplantation report 2020—focus on deceased donor characteristics. J Heart Lung Transplant 2020;39(10):1016–1027.
67. Castañer E, Alguersuari A, Gallardo X, et al. When to suspect pulmonary vasculitis: radiologic and clinical clues. RadioGraphics 2010;30(1):33–53.
68. Salameh M, Grewal J. Pulmonary Tumor Microemboli: A Rare Cause of Dyspnea. J Hosp Med 2008;3(suppl 1):171. https://shmabstracts.org/abstract/pulmonary-tumor-microemboli-a-rare-cause-of-dyspnea/.
69. Ak AK, Mantri SN. Lymphangitic Carcinomatosis. Treasure Island, Fla: StatPearls, 2020.
70. Crane R, Rudd TG, Dail D. Tumor microembolism: pulmonary perfusion pattern. J Nucl Med 1984;25(8):877–880.
71. Dickson AM. The focal hepatic hot spot sign. Radiology 2005;237(2):647–648.
72. Ryu SW, Waugh A, Allman KC. Portosystemic shunting in superior vena cava obstruction by tumor demonstrated on ventilation-perfusion lung scan. J Nucl Med Technol 2014;42(2):118–119.
73. Reed MD, Markov G, Finlay MD, Aisbett KR, Better N. Unusual ventilation-perfusion scintigraphy in adult respiratory distress syndrome secondary to acute lupus myocarditis. Clin Nucl Med 2004;29(12):831–833.
74. Gaur P, Dunne R, Colson YL, Gill RR. Bronchopleural fistula and the role of contemporary imaging. J Thorac Cardiovasc Surg 2014;148(1):341–347.
75. Ono CR, Tedde ML, Scordamaglio PR, Buchpiguel CA. Pulmonary inhalation-perfusion scintigraphy in the evaluation of bronchoscopic treatment of bronchopleural fistula. Radiol Bras 2018;51(6):385–390.